FINNISH METEOROLOGICAL INSTITUTE
CONTRIBUTIONS

No. 125

EFFECTS OF BLACK CARBON AND ICELANDIC DUST ON SNOW ALBEDO, MELT AND DENSITY

OUTI MEINANDER

Finnish Meteorological Institute
Helsinki, Finland

University of Helsinki
The Doctoral Program in Atmospheric Sciences ATM-DP
Department of Environmental Sciences
Faculty of Biological and Environmental Sciences
Helsinki, Finland

Academic Dissertation in Environmental Sciences

To be presented, with the permission of the Faculty of Biological and Environmental Sciences of the University of Helsinki, for public criticism in Auditorium Brainstorm (Erik Palménin aukio 1) on 18 November, 2016, at 12 o'clock noon.

Helsinki, 2016

Supervisors	Professor Gerrit de Leeuw Climate Research, Finnish Meteorological Institute, Finland Department of Physics, University of Helsinki, Finland
	Professor Pekka Kauppi Department of Environmental Sciences University of Helsinki, Finland
Mentor	Dr. Terhikki Manninen Meteorological Research Finnish Meteorological Institute, Finland
Thesis advisory committee	Professor Ari Laaksonen Climate Research Finnish Meteorological Institute, Finland
	Docent Heikki Lihavainen Atmospheric Composition Research Finnish Meteorological Institute, Finland
	Dr. Pavla Dagsson-Waldhauserova Faculty of Environmental Sciences, Agricultural University of Iceland Institute of Earth Sciences, University of Iceland Faculty of Physical Sciences, University of Iceland, Iceland Faculty of Environmental Sciences, Czech University of Life Sciences, Czech Republic
Pre-examiners	Professor Pauline Stenberg Department of Forest Sciences University of Helsinki, Finland
	Professor Lars Eklundh Department of Physical Geography and Ecosystem Science Lund University, Sweden
Custos	Professor Pekka Kauppi Department of Environmental Sciences University of Helsinki, Finland
Opponent	Professor Tiit Nilson Department of Remote Sensing Tartu Observatory, Estonia

Finnish Meteorological Institute Contributions No. 125
ISBN 978-951-697-895-9 (paperback)
ISSN 0782-6117 Finnish Meteorological Institute Contributions
Erweko
Helsinki 2016

ISBN 78-951-697-896-6 (pdf)
http://ethesis.helsinki.fi
Published also by the University of Helsinki in Unigrafia Oy, Helsinki 2016.

FINNISH METEOROLOGICAL INSTITUTE

Published by: Finnish Meteorological Institute (Erik Palménin aukio 1), P.O. Box 503 FIN-00101 Helsinki, Finland

Series title, number and report code of publication: Finnish Meteorological Institute Contributions 125, FMI-CONT-125

Author: Outi Meinander

Date: October 2016

Title

Effects of black carbon and Icelandic dust on snow albedo, melt and density

Abstract

Light-absorbing impurities in the cryosphere are of hydrological, environmental and climatic importance. The wet and dry deposition of black carbon (BC), organic carbon (OC), and dust particles affect the optical properties and melt of snow and ice. In the Arctic region, the climatic effects are amplified, and surface albedo feedback is often cited as the main contributor.

The aim of this thesis is to fill in some of the gaps in our knowledge of the effects of BC, OC, and Icelandic dust on snow in the European Arctic through a series of field and laboratory experiments and an analysis of the resulting data, including modeling. The thesis presents a new hypothesis on the snow density effects of light-absorbing impurities, an important quantity for climate modeling and remote sensing. Three processes are suggested to explain the proposed ”BC density effect”. Experimental results show that dirty snow releases melt water quicker than cleaner snow.

The albedo of natural seasonally melting snow in Sodankylä, north of the Arctic Circle, is found to be asymmetric with respect to solar midday, thus indicating a change in the properties of the snow. The radiative transfer modeling results show that the observed solar zenith angle asymmetry results in a 2–4 % daily error for satellite snow albedo estimates. Surface albedo model results indicate that the biggest snow albedo changes due to BC are expected in the ultraviolet (UV) part of the electromagnetic spectrum. The albedo of natural seasonal snow measured in Sodankylä, is found to be lower than expected. Solar UV and visible (VIS) albedo values of 0.6–0.8 in the accumulation period and 0.5–0.7 during melting are observed. The low albedo values are explained to be due to large snow grain sizes up to ∼3 mm in diameter, meltwater surrounding the grains and increasing the effective grain size, and absorption caused by impurities in the natural snow (87 ppb BC and 2894 ppb OC). The BC contents of the surface snow layer at the Sodankylä Arctic Research Center, Finland, is higher than expected. Increased BC in spring time suggests surface accumulation of hydrophobic BC during snow melt. Some of the high BC concentrations are related to anthropogenic soot transported from the Kola Peninsula, Russia. The origin of OC can be anthropogenic or natural, and may include pollen, seeds, lichens, natural litter or microorganisms that reside in snow and ice.

Iceland is the most important Arctic dust source, but a scientific assessment of its impacts on the cryosphere is currently unavailable and scientific results are urgently needed to investigate the role of Icelandic dust in Iceland and elsewhere, in the past, present and future. Experimental results on Icelandic volcanic ash show that a thin layer increases the snow and ice melt but that an ash layer exceeding a certain critical thickness causes insulation.

The Arctic results of this thesis have relevance to the assessment of Arctic climate change, including modeling and satellite applications.

Publishing unit

Finnish Meteorological Institute, Research and Development, Climate Research

Classification (UDC): 502.3/.7, 504, 550.3

Keywords: Arctic, aerosol, black carbon, Iceland, dust, albedo, snow, ice

ISSN and series title: 0782-6117 Finnish Meteorological Institute Contributions

ISBN: 978-951-697-895-9 (paperback), 78-951-697-896-6 (pdf)

Language: English

Pages: 122

ILMATIETEEN LAITOS

Julkaisija	Julkaisun sarja, numero ja raporttikoodi
Ilmatieteen laitos (Erik Palménin aukio 1) PL 503, 00101 Helsinki	Finnish Meteorological Institute Contributions 125, FMI-CONT-125
Tekijä	Julkaisuaika
Outi Meinander	Lokakuu 2016

Nimeke

Mustan hiilen ja Islannin pölyn vaikutukset lumen heijastavuuteen, sulamiseen ja tiheyteen

Tiivistelmä

Valoa absorboivien partikkeleiden kuiva- ja märkälaskeuma lumen tai jään pinnalle vaikuttaa lumipeitteen optisiin ominaisuuksiin ja sulamiseen ja on tärkeä hydrologian, ympäristön ja ilmaston kannalta. Arktisella alueella ilmastovaikutukset korostuvat etenkin lumen heijastavuuden ja sulamisen takaisinkytkentä-mekanismin takia.

Tämän väitöskirjan tavoitteena on mittaus- ja mallitulosten avulla tuottaa uutta tietoa noen (BC) ja orgaanisen hiilen (OC), sekä Islannin vulkaanisen pölyn laskeuman vaikutuksista Arktisen lumen sulamiseen ja optisiin ominaisuuksiin. Työssä esitetään uusi hypoteesi, jonka mukaan valoa absorboivat hiukkaset voivat vähentää sulavan pintalumen tiheyttä, joka on tärkeä ilmastomallien ja lumen satelliittimittausten muuttuja. Tätä selitetään kolmella mahdollisella prosessilla.

Sodankylässä vuotuisen lumipeitteen heijastuskyky (albedo) oli lumen sulamiskaudella alhaisempi kuin kirjallisuuden perusteella osattiin odottaa. Lumen ultraviolettisäteilyn (UV) ja näkyvän valon (VIS) heijastuskyky oli 0.6–0.8 talviaikaan ja 0.5–0.7 sulamiskaudella. Alhaista albedoa selittävät lumen suuri kidekoko ja kidettä ympäröivä sulamisvesi, sekä lumen valoa absorboivat epäpuhtaudet (87 ppb nokea ja 2894 ppb orgaanista hiiltä). Sodankylän Arktisen tutkimuskeskuksen pintalumen mustan hiilen pitoisuudet olivat odotettua (< 60 ppb) suuremmat. Nokea kertyi lumen pintakerrokseen lumen sulaessa. Toinen syy korkeisiin nokipitoisuuksiin oli kaukokulkeuma lähialueilta. Orgaaninen hiili voi olla peräisin orgaanisten yhdisteiden päästöistä tai se voi koostua luonnollisista lumelle kertyneestä tai siinä kasvavasta orgaanisesta materiaalista, kuten neulaset, siitepölyhiukkaset, siemenet, sienirihmat, jäkälät ja levät.

Sulamiskaudella lumen heijastuskyky oli auringon korkeuskulman funktiona epäsymmetrinen, koska lumen fysikaalisten ominaisuuksien muuttuminen päivän mittaan vaikutti albedoon. Säteilynkuljetusmallilaskelmat osoittivat, että tämä epäsymmetria voi aiheuttaa 2–4 % virheen satelliittimittausten perusteella tehtyihin albedoarvoihin. Pinta-albedon mallilaskelmat osoittivat, että noki vähentää lumen heijastuskykyä sitä enemmän mitä lyhyempi säteilyn aallonpituus on kyseessä ja eniten ihmissilmälle näkymättömillä UV-säteilyn aallonpituuksilla.

Arktisella alueella Islannin pöly voi olla merkittävä lumen sekä jään ja jäätiköiden optisten ominaisuuksiin ja sulamiseen vaikuttava tekijä, ja mahdollisesti yhtä suuri tai jopa tärkeämpi kuin noki. Tutkimustuloksia on toistaiseksi hyvin vähän. Tässä työssä havaittiin, että ohut tuhkakerros edisti lumen ja jään sulamista, mutta suurempi määrä toimi eristeenä ja hidasti sulamista.

Väitöskirjan tuloksia voidaan hyödyntää Arktisen alueen ilmastonmuutoksen arvioinnissa, mukaan lukien mallinnus- ja satelliittisovellutukset.

Julkaisijayksikkö

Ilmatieteen laitos, Tutkimus ja menetelmäkehitys, Ilmastotutkimus

Luokitus (UDK)	Asiasanat
502.3/.7, 504, 550.3	Arktinen, aerosoli, Islanti, musta hiili, orgaaninen hiili, lumi, jää, albedo

ISSN ja avainnimike

0782-6117 Finnish Meteorological Institute Contributions

ISBN

978-951-697-895-9 (nid.), 78-951-697-896-6 (pdf)

Kieli	Sivumäärä
englanti	122

Prewords

This thesis work on light-absorbing particles in snow completes my postgraduate Phil.Lic. university degree into PhD, more recognized internationally. However, I am also aware that it is important to avoid using "Dr." when, e.g., booking flight tickets ("Is there a doctor on board this flight?")…the best memories are thanks to many people! I want to thank my co-authors of the original publications included in this thesis, Pavla, Anna, Terhikki, Mona (and her co-authors), Kaisa, Anu, Hanne, Oli, Aki, Antti, Matti, Aku, Jonas, Stelios, Petri, Roux, Michael, Leif, Jean-Louis, Olivier, Lasse, Onni, Rigel, Veijo, Martti, and Gerrit. Special thanks to Gerrit for his support and supervision of my thesis, and Terhikki for kindly mentoring me. I also thank Pekka Kauppi, my supervisor from the University of Helsinki, for his help. I am most grateful for all the supportive people surrounding me, including my family and friends.

Prof. Steven Warren, University of Washington, USA, I thank for his guidance on BC in snow while in Norway, and Dr. Sarah Doherty for the BC analysis of some of my snow samples. In addition to the co-authors, recent collaboration and great discussions and future plans have taken place thanks to many people, especially prof. Olafur Arnalds; prof. Joe Prospero; prof. Zhijun Li; as well as Maria Gritsevich, Jouni Peltoniemi, Timo Nousiainen, and many other colleagues. I also want to acknowledge Liisa Jalkanen, who initially employed me as a summer worker for the FMI Chemistry laboratory, and prof. Juhan Ross I remember for his positive supervision. For many years, my practical work at FMI was part of prof. Esko Kyrö's Antarctic-Arctic research, thank you Esko and thanks to all Marambio collaborators! Timo Vihma I thank for his supervision of my Antarctic Thesis for MetPD (meteorology), and Roberta Pirazzini for sharing her experiences in the Antarctic snow research. The FMI Snow Team of Kirsti Kylhä, the members of COST SNOW ES1404 of Ali Nadir Arslan, our '553research group', and Antti Aarva and Sodankylä personnel, as well as the morning-coffee table (most often Laura, Tiina, Kirsi, Simo and Leif), deserve to be mentioned.

The members of the thesis advisory committee (Pavla, Ari and Heikki), as well as prof. Pauline Stenberg and prof. Lars Eklundh (pre-examiners of this thesis) I gratefully thank for their valuable comments on the thesis draft. Prof. Tiit Nilson I thank for accepting to be my opponent. Finally, I want to thank Dr. Yrjö Viisanen, our R&D director, prof. Jouni Pulliainen, our Sodankylä Arctic Center director, and Dr. Juhani Damski, FMI Director-General, for the excellent working conditions and scientific environment provided at FMI. This thesis was prepared at FMI within the ATM-DP, FCoE ATM and NCoE CRAICC of the University of Helsinki, prof. Markku Kulmala. I am thankful for this support.

Sometimes research work has challenges similar to those faced by the crew onboard the Starship Enterprise (Star Trek series, which belongs to my favorites), but more surprisingly some imagination things from Start Trek have recently become realistic, too: let's consider a food replicator vs 3D-printing, and holodeck vs the Finnish invention of SmogScreen! That makes me wonder: When can we be beamed up and energized? While waiting for that to happen, let's set a course to the Arctic. These are the voyages.

Helsinki, October 2016, Outi Meinander

Contents

List of original publications and author's contribution

This thesis consists of an introductory overview, followed by five research articles. In the introductory part, these papers are cited according to their roman numerals PAPER I–V.

I Meinander, O., Kontu, A., Lakkala, K., Heikkilä, A., Ylianttila, L., and Toikka, M.: Diurnal variations in the UV albedo of Arctic snow, Atmos. Chem. Phys., 8, 6551-6563, doi:10.5194/acp-8-6551-2008, 2008.

II Meinander, O., Kazadzis, S., Arola, A., Riihelä, A., Räisänen, P., Kivi, R., Kontu, A., Kouznetsov, R., Sofiev, M., Svensson, J., Suokanerva, H., Aaltonen, V., Manninen, T., Roujean, J.-L., and Hautecoeur, O.: Spectral albedo of seasonal snow during intensive melt period at Sodankylä, beyond the Arctic Circle, Atmos. Chem. Phys., 13, 3793-3810, doi:10.5194/acp-13-3793-2013, 2013.

III Meinander, O., Kontu, A., Virkkula, A., Arola, A., Backman, L., Dagsson-Waldhauserová, P., Järvinen, O., Manninen, T., Svensson, J., de Leeuw, G., and Leppäranta, M.: Brief communication: Light-absorbing impurities can reduce the density of melting snow, The Cryosphere, 8, 991-995, doi:10.5194/tc-8-991-2014, 2014.

IV Dragosics, M., Meinander, O., Jónsdóttír, T., Dürig, T., De Leeuw, G., Pálsson, F., Dagsson-Waldhauserová, P., and Thorsteinsson, T.: Insulation effects of Icelandic dust and volcanic ash on snow and ice. Arabian Journal of Geosciences, 9, 126, doi: 10.1007/s12517-015-2224-6, 2016.

V Meinander, O., Dagsson-Waldhauserova, P., and Arnalds, O.: Icelandic volcanic dust can have a significant influence on the cryosphere in Greenland and elsewhere. Polar Research, 35, 31313, doi:10.3402/polar.v35.31313, 2016.

O. Meinander was responsible for the PAPER I–III and V. She planned the contents of the PAPER I–II, invited the co-workers needed, and participated in a large part of the work and data-analysis and writing, except the SILAM modeling calculations. In PAPER III, she created the hypothesis; the reasons for the density effects were formulated by all the co-authors as a team. For PAPER IV, O. Meinander was responsible for planning and supervising the work and manuscript writing of PhD student M. Dragosics at the Institute of Earth Sciences, University of Iceland. For PAPER V, she was the initiator of the paper and responsible for planning the contents and arguments presented, with contributions from the other co-authors.

Abbreviations

AMAP	Arctic Monitoring and Assessment Programme
ARC	Arctic Reserach Center
AWS	Automated Weather Station
BB	Broadband
BC	Black Carbon
BHR	Bihemispherical Reflectance
BRDF	Bidirectional Reflectance Distribution Function
BRF	Bidirectional Reflectance Factor
DP	Doctoral Program
EC	Elemental Carbon
EM	Electromagnetic
ET	Extraterrestrial
FCoE	Finnish Center of Excellence
FMI	Finnish Meteorological Institute
GAW	Global Atmospheric Watch
IPCC	Intergovernmental Panel of Climate Change
IPY	International Polar Year
LAI	Light Absorbing Impurity
LAP	Light Absorbing Particle
LW	Longwave
MAC	Mass Absorption Cross section
MBFR	Multiband Filter Radiometer
MODIS	Moderate Resolution Imaging Spectrometer
NASA	National Aeronautics and Space Administration
NCoE	Nordic Center of Excellence
NIR	Near Infrared
OC	Organic Carbon
PEEX	Pan-Eurasian Experiment
PM	Particulate Matter
RT	Radiative Transfer
SLCF	Short-Lived Climate Forcer
SMEAR	Station for Measuring Ecosystem-Atmosphere relations
SNICAR	Snow, Ice, and Aerosol Radiation -model
SNORTEX	Snow Reflectance Transition Experiment
SW	Short Wave
UV	Ultraviolet
VIS	Visible
WMO	World Meteorological Organization
WOUDC	World Ozone and Ultraviolet Data Center, Canada

1 Introduction

1.1 Background

Atmospheric aerosols are small (3 nm – 100 μm) liquid or solid particles suspended in the atmosphere. These particles originate from various natural and anthropogenic sources. Aerosol species include sulfates, sea salt, nitrates, organic carbon, black carbon, ash, and wind-blown dust. They can be directly emitted into the atmosphere, or formed (from precursor gases) through chemical and physical processes, and they are capable of being long-range transported. The atmospheric residence time of aerosol particles ranges from hours for coarse particles towards days (or weeks) for fine mode particles (< 1 μm). The residence time of fine mode particles is significantly shortened by wet deposition. The properties of the particles can be described based on their shape, size, and chemical composition. A significant feature of aerosol particles is their ability to scatter and absorb atmospheric solar radiation. Light-absorbing aerosol particles include soot (black carbon, BC), ash, dust, and the so called brown-carbon fraction of organic carbon (OC).

In the cryosphere, light-absorbing particles (LAP) are of hydrological, environmental, and climatic importance, depending of their physical and chemical properties. When deposited on snow and ice surfaces, the climatic effects of dark particles are due to reduced albedo and induced melt of darker surfaces, which again lowers the albedo and increases melt via the albedo feedback mechanism (Arrhenius 1896, Warren and Wiscombe 1980, Doherty et al. 2010). In the Arctic region, these climatic effects are amplified, and the surface albedo feedback is often cited as the main contributor to a phenomenon known as Arctic amplification, referring to greater warming in the Arctic compared to the global average (Arrhenius 1896, Serreze and Barry 2011, Pithan and Mauritsen 2014). Currently, Arctic amplification is understood to have a variety of causes on different temporal and spatial scales, including the albedo feedback, retreat of sea ice, changes in atmospheric and oceanic heat fluxes, changes in cloud cover and water vapor content, soot on snow, and heat absorbing BC aerosols in the atmosphere (Serreze and Barry 2011). Darkening and melt effects are most often linked to BC, but OC and dust can have similar effects. In addition to deposited atmospheric particles, cryospheric light-absorbing impurities (LAI) may consist of natural organic litter like needles, pebbles, and various microorganisms that reside in snow and ice.

The sources for BC are mainly incomplete combustion of carbonaceous material, like fossil fuels and biomass. In the Arctic, BC originates from emissions from industrial and biofuel burning, mostly from long-range transported extra-Arctic emissions from Europe, North America, Former Soviet Union and East Asia (Sharma et al. 2013, Jiao et al. 2014). The BC emissions of China and India have been evaluated among the largest of the Asian BC hot-spot region (Wang et al. 2014). Gas flaring can also be a significant source at high

latitudes (Stohl et al. 2013). Koch and Hansen (2005) say that half of biomass-originating BC in the Arctic comes from north of 40^{o}N (North America, Russia, and Europe, each contributing 10–15 %). They also report that Russia, Europe, and south Asia each contribute about 20–25 % of BC to the low-altitude springtime ‘‘Arctic haze”, which consists primarily of anthropogenic particles with high sulfur concentrations and other components such as soot.

BC can affect the Arctic climate through several mechanisms. These include direct heating of the Arctic atmosphere (Ramanathan and Carmichael 2008), darkening and increased melt of Arctic snow and ice (Hansen and Nazarenko 2004, Flanner et al. 2007, Bond et al. 2013), alteration of Arctic cloud shortwave and longwave properties and cloud formation (Koch and Del Genio 2010), and perturbation of the poleward heat flux through forcing exerted outside the Arctic (AMAP 2015). Arctic climate response has been found sensitive to the vertical distribution and deposition efficiency of BC reaching the Arctic (Flanner 2013). The Intergovernmental Panel on Climate Change Fifth Assessment Report (IPCC 2013) assesses the BC on snow/ice to have a global and annual mean direct radiative forcing of 0.40 Wm^{-2}. BC emissions occurring within the Arctic have been found to induce about fivefold greater warming, normalized to the mass of emissions, than emissions from mid-latitudes, because a higher fraction of within-Arctic emissions deposit to snow and sea ice than mid-latitude emissions (Sand et al. 2013). The role of BC in snow and ice has been widely investigated, and detailed scientific assessments have been presented in Bond et al. (2013), IPCC (2013), and AMAP (2015).

Black carbon is a Short-Lived Climate Forcer (SLCF) and it undergoes regional and intercontinental transport from source regions during its short atmospheric lifetime. Atmospheric removal of BC occurs within a few days to weeks via precipitation and contact with surfaces (Bond et al. 2013). The life time of BC can be largely determined by factors that control local deposition rates, e.g., precipitation (Zhang et al. 2015). Wet-scavenging processes (in-cloud and below-cloud scavenging) are a major source of uncertainty in predicting atmospheric BC concentrations over remote regions (Schwarz et al. 2010). When emitted, BC is mostly hydrophobic (Laborde et al. 2013) but can become coated with water-soluble components through atmospheric aging processes, where BC changes from hydrophobic to hydrophilic. Aerosols can also form complex mixtures. For example, soot particles can mix with nitrates and sulfates, or they can coat the surfaces of dust.

The main sources of OC aerosols, co-emitted in the atmosphere with BC, are anthropogenic activities and wildfires (e.g., Hegg et al. 2010). Bond et al. (2013) mention that a large fraction of particulate light absorption in Arctic snow (about 30 to 50 %) is due to non-BC constituents and most of the absorption would be due to light-absorbing OC, called brown carbon. Different types of brown carbon can include coal combustion, biomass burning, organic compounds emitted from local soils, and volatile organic compounds (VOC) emitted by vegetation. France et al. (2012) explained that BC alone could not account for all the absorption seen in the Barrow snowpacks, and an additional absorption by Humic Like Substances (HULIS, part of brown carbon), and other chromophores was necessary to explain the observed variation. Voisin et al. (2012) measured HULIS optical properties and reported them to be consistent with aged biomass burning or a possible marine source. McNeill et al. (2012) discussed the adsorption and

desorption of organic species to and from snow and ice surfaces, and how these processes influence the transport of organic trace gases through the snowpack. A much higher OC to EC ratio (205:1) was reported for snow than in air (10:1), indicating that snow would be additionally influenced by watersoluble gasphase compounds (Hagler et al. 2007). According to AMAP (2015), in case of using the thermo-optical analysis method for OC in snow, pieces of organic material, such as bits of leaf or twig, can contribute significantly to the OC results. Cryoconite (a mixture of dust, pebbles, soot, and microbes) (Tedesco et al. 2015) and color-pigmented algae (Benning et al. 2014, Lutz et al. 2016) have been added in the discussions on snow darkening and melt more recently, especially in Greenland. In the melting of glaciers (glaciar snow melt), the role of BC is considered uncertain, because few measurements of glacial BC content exist, and the impact of natural impurities, such as soil dust and algae, has not sufficiently been accounted for (Bond et al. 2013).

Dust is a major environmental factor in the Earth system with important impacts on global energy and carbon cycles. Atmospheric desert dust particles are soil particles suspended in the atmosphere from regions of dry unvegetated soils with erosion and strong winds. Because of its effects from timescales of minutes (as with dust devils, cloud processes and radiation) to millennia (as with oceanic sediments, and loess sediments formed by the accumulation of wind-blown silt), dust is not only a key environmental player, but also a recorder of environmental change (Knippertz & Stuut 2014). The multiple processes in which dust takes part include dust interaction with continental and marine ecosystems by being a source of micronutrients; when deposited in the cryosphere, dust changes the amount of reflected solar radiation; dust affects the solar radiation in the atmosphere and properties of clouds and thereby also precipitation. Studies show that at low and mid-latitudes, Saharan dust can affect the albedo and long-term mass balance of an Alpine glacier (Di Mauro et al. 2015, Gabbi et al. 2015). Dust from Asian deserts is deposited on Himalayan snow resulting in darkening and increased snow melt (Gautam et al. 2013). Mineral dust from the Colorado Plateau can shorten snow cover duration of the San Juan Mountain range (Painter et al. 2007). Recently, it has been recognized that dust produced in high latitude and cold environments may have regional or global significance (Bullard et al. 2016). Dust is included in the IPCC (2013) report as an anthropogenic source due to the development of agriculture which favors the generation of dust.

In the Arctic region, Iceland is the most active dust source (Arnalds et al. 2016). The dust day frequency in Iceland is similar to that in the major desert areas of the world (Mongolia, Iran, USA, China). Frequent volcanic eruptions with the re-suspension of volcanic materials and dust haze increase the number of dust events fourfold, resulting in 135 dust days in Iceland annually (Dagsson-Waldhauserova et al. 2014). High-latitude dust transport over the North Atlantic with inputs from Icelandic dust storms was described for the first time by Prospero et al. (2012). About 50 % of the annual dust events in the southern part of Iceland take place at sub-zero temperatures, when volcanic dust may be mixed with snow (Dagsson-Waldhauserova et al. 2015). There are over 30 active volcanoes or volcanic systems in Iceland, and seven major dust sources (Arnalds 2010, Arnalds et al. 2016). The properties of ash and dust from these sources show considerable physical and chemical variability. Icelandic volcanic dust properties, origin and transport

have been widely investigated (Arnalds et al. 2016), but fewer investigations are available for dust-cryosphere interaction (Dagsson-Waldhauserova 2015, Arnalds et al. 2016).

Figure 1.1. Dark volcanic dust on the surface of an Icelandic glacier. Light-absorbing aerosols, such as black carbon, organic carbon, ash and dust, originate from various natural and anthropogenic sources. When deposited on snow and ice surfaces they reduce the surface albedo and increase melt via the albedo feedback mechanism. Photo O. Meinander, Solheimajökull, Iceland, in March 2016.

This thesis deals with effects of BC, OC and Icelandic volcanic dust on snow and ice properties in the Arctic region, as discussed in connection with sources of emissions, and transport and deposition. For black carbon, different names are used in the literature. Here BC refers to light-absorbing carbonaceous substances when there is no reference to a specific measurement method. Elemental carbon (EC) is used when results refer to the carbon content specific thermo-optical method. Soot is composed mainly of carbon and produced when organic (carbon-containing) material is burned. An individual hydrophobic soot particle is composed of graphitic layers and has a typical diameter of 45 nm (AMAP 2015). Volcanic dust (Figure 1.1) is defined as any volcanic material which is re-suspended from old deposits of any volcanic material, regardless of age and mode of formation (Dagsson-Waldhauserova et al. 2015). According to AMAP (2015), there is no fixed definition for the Arctic, and the term Arctic is there used for latitudes North of 60°N. More often, the Arctic is defined as the area north of the Polar Circle. In case of Iceland, Arctic dust events have been used to refer to NE Icleand, and Sub-Arctic dust events to S Iceland (Dagsson-Waldhauserova et al. 2014). Here the Arctic results refer mainly to Arctic Finland (PAPER I–III) and Iceland (PAPER III–V), but also to the Arctic

region more broadly (PAPER V). Due to the lack of standardization of reflectance terminology (Shaepman-Strub et al. 2006), this thesis uses notations following Shaepman-Strub et al. (2006). Albedo is defined as bihemispherical reflectance (BHR). For clarity, spectral albedo (BHR_{λ}) is distinguished from the eryhemally weighted broadband albedo (BHR_{ery}). The term light-absorbing refers to the electromagnetic radiation at 300–2500 nm.

In the next section 1.2, I will identify the scope, research questions and objectives of the thesis. The main gaps of knowledge and open research questions at the time this research was conducted, which this thesis addresses, are also presented in section 1.2. This is followed by describing the outline of the thesis in section 1.3. Thereafter, theory and scientific knowledge of effects of light-absorbing impurities will be introduced in section 2. Then chapters on materials and methods, and overview of results and discussion, will be presented. The thesis is completed with summary and conclusions, and plans for future work.

1.2 Scope, research questions and objectives

The aim of this thesis is to fill in some of the gaps in our knowledge and understanding of the impacts of the light-absorbing aerosols of BC, OC, and Icelandic volcanic dust, on the snow and ice albedo, melt and density, especially in the Arctic. Such effects are of hydrological, environmental and climatic importance via surface darkening and increased snow melt. The thesis contributes with new continuous Arctic measurement data, field campaigns, and laboratory experiments since the International Polar Year (IPY) 2007/2008, for the data-sparse region in the Arctic, in the Northern Europe. The work started with the Sodankylä snow ultraviolet (UV) albedo measurements (initiated during IPY 2007/2008, PAPER I), continued including effects of BC/OC on Sodankylä snow (PAPER II), a hypothesis on BC density effects (PAPER III), effects of Icelandic dust (PAPER IV), and the role of Icelandic dust in the Arctic cryosphere more broadly (PAPER V). The thesis also includes some Arctic-Antarctic aspects, and discusses some of the challenges and possibilities in modeling and satellite approaches.

When the work on Sodankylä snow started with the continuous in situ UV albedo measurements (PAPER I–II), this was the first of its kind in Finland; only the UV irradiance and VIS albedo (at visible wavelengths) were included in the atmospheric radiation measurements of the Finnish Meteorological Institute (FMI). Earlier, UV albedo measurements had been made elsewhere in the Arctic and Antarctic (Smolskaia et al. 1999, Perovich et al, 2002, Pirazzini 2004, Wuttke et al. 2006). The Snow UV albedo is of importance as it amplifies the amount of the surface UV radiation. The stratospheric ozone depletion increases the UV irradiance reaching the ground, too. The UV radiation has many positive and negative impacts. The UV albedo of snow can be the reason behind a painful eye condition known as snow blindness (UNEP 2002). The UV radiation is needed for the vitamin D production and it has a harmful effect on causing DNA damage and skin cancer (WHO 2006), as well as material degradation (Andrady et al. 2015, Heikkilä 2014), and it is important in air chemistry in photolysis reactions. Estimates on the snow UV

albedo were used for satellite UV algorithms in Arola et al. (2003), and Tanskanen and Manninen (2007). The snow UV albedo measurements in Sodankylä were initiated during IPY 2007/2008, and investigated then with the help of ancillary meteorological and snow information (PAPER I). Later (PAPER II-V), the work included snow albedo, melt and density investigations linked to atmospheric particles deposited in snow, which is of particular interest due to the UV absorbing properties of some of the aerosol particles.

The albedo effects of dirty snow were first published by Warren and Wiscombe (1980). Their results are currently in use in the snow albedo model SNICAR (Flanner et al. 2007), acknowledged and used by the IPCC (2013), too. Recently, more than 30 years later, an empirical dataset on impurities in Arctic snow were made available by Doherty et al. (2010). Their investigation updated the 1983–1984 survey of Clarke and Noone (1985). The work of Doherty et al. (2010) covered BC in snow in Alaska, Canada, Greenland, Svalbard, Norway, Russia, and the Arctic Ocean, but no snow samples from Finland were included. Their closest place was Tromso, Norway, which represented the European Arctic. In 2013, Svensson et al., Forsström et al. and PAPER II reported BC concentrations in snow samples collected in the European Arctic snowpacks.

Next, I will identify the contribution of the PAPER I–V to different scientific questions and objectives. The specific research questions, to which answers were searched for in this thesis, were as follows:

Q1: What is the in situ snow UV albedo in Sodankylä, north of the Arctic Circle and why? (= Objective of the PAPER I–II)

Q2: How much BC and OC is there in seasonal snow in Sodankylä and why? (= Objective of the PAPER II)

Q3: Why does dirty snow melt faster than clean snow, i.e., what happens after impurities absorb radiation and snow melt starts? (= Objective of the PAPER III)

Q4: How does Icelandic volcanic dust interact with snow and ice and why, and what are the potential impacts of Icelandic dust? (= Objective of the PAPER IV–V)

Q5: What are the challenges, needs and possibilities in modeling and remote-sensing approaches and in bipolar Arctic-Antarctic research? (= Objectives of the PAPER I, II and V).

In this thesis work, these research questions related to effects of elemental carbon, organic carbon, and Icelandic volcanic dust, on snow and ice optical properties, melt and density have been investigated. Various approaches were used, as will be explained in the Chapter 3.

1.3 Outline of the thesis

The thesis consists of five original papers. These are referred to by roman numbers (PAPER I–V). The contributions of PAPER I–V to the thesis are presented in Table 1.1. The focus of PAPER I–II is on the snow albedo and reflectance, and BC/OC in natural Arctic Sodankylä snow. PAPER III presents a new hypothesis on the snow density

effects. PAPER IV shows experimental data where snow melt increases for smaller amounts of Icelandic dust particles in snow, and insulation can take place in case of thicker dust layers. PAPER V states that the scientific assessment of impacts of Icelandic dust in cryosphere is currently missing, urges for scientific investigation, and hypothesizes that in the Arctic Icelandic dust can have similar or larger albedo and melt effects on the cryosphere than soot.

Table 1.1. The contribution of PAPER I–V to the thesis.

Subject	PAPER I	PAPER II	PAPER III	PAPER IV	PAPER V
Black carbon		X	X		X
Organic carbon		X	X		X
Icelandic dust			X	X	X
Snow /Ice albedo	X	X	X		X
Snow /Ice melt	X	X	X	X	X
Snow density			X		

The structure of the thesis is planned as follows. In the next chapter, the theoretical and scientific literature of light-absorbing impurities and cryosphere is described, with the focus in Arctic. The materials and methods are presented in Chapter 3 and the Chapter 4 contains an overview of the main results and their discussion based on the original papers. The synthesis includes effects of BC, OC, and Icelandic volcanic dust on the snow and ice albedo, melt and density, as well as modeling and remote sensing related aspects. Conclusions and future aspects are included in Chapters 5–6.

2 Light-absorbing particles in the Arctic snow

Light-absorbing atmospheric particles deposited in snow cause changes in the interaction of solar irradiance and snow. According to the law of energy conservation, the incoming solar radiation can be absorbed, reflected or transmitted. A change in any of these components can therefore be used to indicate changes in the properties of the target under investigation. Clean non-melting snow reflects generally 80–90 % of the incident solar radiation (Wiscombe and Warren 1980). Darker, dirty snow absorbs more solar radiation, decreasing snow reflectivity (Warren and Wiscombe 1980). This in turn increases snow melt, which again decreases the reflectance of snow. This is known as the snow albedo feedback mechanism. Hence, in the presence of light-absorbing particles in snow, the key driving force for snow melt is the decrease in snow reflectivity. In addition, for the surface radiation balance, changes in snow surface reflectivity are most critical. As the irradiation that is reflected back to space does not heat the Earth, snow cover cools the climate both locally and globally and is an important factor in the global energy balance. The climatic affects are amplified in the Arctic. In this chapter, we first take a look on the theory to understand what light is (section 2.1), and what controls the solar irradiance at the Earth surface (section 2.2), where after factors affecting the snow bihemispherical reflectance, i.e. albedo, of clean and dirty snow are presented (section 2.3).

2.1 Electromagnetic radiation

Light is electromagnetic radiation, whose main source in the Earth is the Sun. According to the wave model of electromagnetic radiation, the solar spectral irradiance $E(\lambda)$ consists of wavelengths from 100 to 5000 nm (Harris 1987). The term spectral is used when the wavelength dependency is being described. Electromagnetic waves are often categorized by their location within the electromagnetic spectrum. For example, electromagnetic radiation at 300–400 nm is called ultraviolet (UV) radiation, at 400–700 nm visible (VIS) radiation, and at 700–2500 nm near-infrared (NIR) radiation. Light most often refers to light visible to human eye in the wavelength range of 400–700 nm. It should be noted that only thermal IR is directly related to the sensation of heat, while NIR is not. Because of the similarity in the behavior of UV, VIS and NIR regions of the spectrum, they are all incorporated in the field of physical research known as optics. In ecophysiology, agriculture, forestry and oceanography, the waveband between 400–700 nm contains what is known as photosynthetically active radiation (PAR). In addition to the wave model,

electromagnetic radiation is, according to the particle theory, composed of many discrete units called photons or quanta. The wave and quantum models of electromagnetic radiation are related by the equation

$$Q = h\,f = \frac{hc}{\lambda} \tag{2.1}$$

where Q = energy of a quantum [J]; h = Planck's constant, 6.626×10^{-34} [J sec]; f = frequency [s^{-1}]; c = velocity of light, 299792458 [m/s]; and λ = wavelength [m].

Only 2 % of the radiated extraterrestrial (ET) solar energy corresponds to the wavelength range below 220 nm and 3 % above 2700 nm (Agrawal 1986).

2.2 Solar irradiance at the Earth surface

Due to the absorption and scattering properties of the Earth's atmosphere, only part of the ET solar spectral irradiance is passed through the atmosphere. Incident solar radiation, i.e., solar irradiance at the Earth's surface, has both direct (sunlight) and diffuse (skylight) components. The direct solar irradiance $E_{dir}(\lambda)$ reaching the Earth surface is regulated by the product of the extraterrestrial spectral irradiance $E_{ET}(\lambda)$ and a wavelength-dependent effective transmission function T (Bird and Riordan 1986):

$$E_{dir}(\lambda) = E_{ET}(\lambda)\ D\ T(\lambda, \theta, \tau_r, \tau_a, \tau_{w,} \tau_{O,} \tau_{u,}) \tag{2.2}$$

where $E_{dir}(\lambda)$ is the direct spectral irradiance on a surface normal to the direction of the Sun at ground level, $E_{ET}(\lambda)$ is the extraterrestrial spectral irradiance at the mean Earth-Sun distance, D is the correction factor for the Earth-Sun distance, θ is the solar zenith angle, and τ_r, τ_a, $\tau_{w,}$ $\tau_{O,}$ τ_u are the transmittance functions of the atmosphere for molecular (Rayleigh) scattering, aerosol attenuation, water vapor absorption, ozone absorption and uniformly mixed gas absorption, respectively.

The direct irradiance on a horizontal surface is obtained by multiplying Eq. (2.2) by $\cos\theta$. The surface albedo is a non-dimensional, unitless quantity that indicates how well a surface reflects solar energy. Albedo values vary between 0 and 1 (0–100 %). The spectral surface albedo is defined as the Bihemispherical Reflectance (BHR_λ), i.e., the ratio of the radiant flux reflected from a unit surface area into the whole hemisphere to the incident radiant flux of hemispherical angular extent as a function of wavelength (Schaepman-Strub et al. 2006):

$$BHR_\lambda = \frac{d\Phi_r(\theta_i, \phi_i, 2\pi, 2\pi, \lambda)}{d\Phi_i(\theta_i, \phi_i, 2\pi, \lambda)} \tag{2.3}$$

where Φ_r is the reflected radiant flux [W/nm], Φ_i is the incident radiant flux [W/nm], and (θ_i,ϕ_i) is the incident solar angle (zenith, azimuth).

In optical remote sensing terms, this definition of the surface albedo is often named as blue-sky albedo. The total diffuse solar irradiance $E_{diff}(\lambda)$ at the Earth surface is a sum (Bird and Riordan 1986) of components of Rayleigh $E_r(\lambda)$ and aerosol scattering $E_a(\lambda)$, and the component $E_g(\lambda)$ that accounts for the multiple reflection of irradiance between the ground and the air:

$$E_{diff}(\lambda) = E_r(\lambda) + E_a(\lambda) + E_g(\lambda) = E_{ET}(\lambda)\ D\ T(\lambda, \theta, \tau_r, \tau_a, \tau_w, \tau_O, \tau_u)\ k(BHR_\lambda, r_{s\lambda}) \qquad (2.4)$$

where $k = BHR_\lambda r_{s\lambda}/(1-BHR_\lambda r_{s\lambda})$; BHR_λ = bihemispherical spectral surface reflectance; $r_{s\lambda}$ = spectral sky reflectivity.

In some research applications it may be assumed that diffuse radiation is isotropic, i.e. has the same intensity regardless of the direction of measurement. The contribution of direct and diffuse components varies according to the solar elevation and wavelength: the smaller the wavelength and the lower the sun, the larger the diffuse component. Under an overcast fully cloudy sky all light is diffuse sky radiation.

Radiation having wavelength smaller than 100 nm (X-rays and Gamma rays) is absorbed in the ionosphere by oxygen molecules (O_2) and free oxygen atoms (O). The ET ultraviolet radiation range is 100–400 nm, but atmospheric absorption of oxygen molecules (O_2) prevents the most harmful UV-C radiation (100–280 nm) from reaching the surface. UV-B radiation (280–315 nm) is strongly absorbed by stratospheric ozone (O_3) with the absorption bands of Hartley (between 200–300 nm, with a maximum absorption at 255 nm), Huggins (weak absorption between 300–360 nm), and Chappuls (weak between 440–1180 nm) (Liou 2002). Carbon dioxide (CO_2) has absorption bands at 2300 and 4500 nm. Water vapor, $H_2O(g)$, has some absorption between 600 and 2000 nm and at 3000 nm.

In addition to the mechanism of atmospheric absorption, particles in the atmosphere cause atmospheric scattering. In general, if the particle is very much smaller in diameter than the wavelength of radiation, 'Rayleigh scattering' dominates. When the diameter of the particle is much larger than the wavelength, geometric 'nonselective scatter' prevails. 'Mie scattering' takes place when atmospheric diameter of the particle is of the order of the wavelength of the incoming radiation. The Mie scattering theory (Mie 1908) assumes homogenous spheres, none of which is a valid assumption for dust. For the non-spherical particles of dust and ash, Mie assumption is thus an error source in the scattering calculations (Nousiainen and Kandler 2015).

Changes in the values of the parameters in the atmospheric transmission function $T(\lambda)$ can be studied by in situ measurements, or radiative transfer (RT) model calculations, or by using satellite data. In the RT equation, the propagation of the electromagnetic radiation through the atmosphere can be described using a rather complicated equation including all the possible directions of propagation, where solar irradiance loses energy to the atmosphere by absorption, gains energy by atmospheric emission, and redistributes energy by scattering. A detailed description of the RT equation is found in Liou (2002),

for example. Often, a simplified two-stream approximation is used, where two directions (streams) of upward ($E\uparrow$) and downward ($E\downarrow$) irradiance are included. The solution of the RT equation generally yields the directional quantities of diffuse and direct irradiances upward and downward. The ratio of all reflected upward (↑) irradiance to the incident downward (↓) irradiance includes the diffuse and the specular radiation reflected.

2.3 Radiation - snow interaction

The solar electromagnetic radiation at wavelengths < 5000 nm is called shortwave (SW) radiation. At longer thermal wavelengths radiation is emitted. For the snow or ice (glacier) surface radiation balance, the net energy flux E_{N} is due to differences between downward (↓) and upward (↑) non-thermal shortwave (SW) and thermal longwave (LW) radiative fluxes, and can be expressed as (Garratt 1992):

$$E_N = E_{SW\downarrow} - E_{SW\uparrow} + E_{LW\downarrow} - E_{LW\uparrow} \tag{2.5}$$

where the net shortwave flux depends on the incident solar radiation and on the surface Bihemispherical Reflectance BHR (albedo), and the net longwave flux depends on the downwelling longwave radiation, the Stefan-Boltzmann constant σ ($5.670373\times10{-}8\mathrm{W\ m^{-2}K^{-4}}$), the surface emissivity ε_s, and the temperature of the surface T_s (in Kelvin):

$$E_N = (1 - \mathrm{BHR})\, E_{SW\downarrow} + E_{LW\downarrow} - \{(1 - \varepsilon_s)\, E_{LW\downarrow} + \varepsilon_s\, \sigma\, T_s^4\} \tag{2.6}$$

This shows that E_N is most critically influenced by the surface characteristics of the BHR (albedo) and emissitivity ε_s. Emissivity ε_s (0–1) is a measure of the thermal emittance of a surface, defined as the ratio of radiant heat flux emitted by a material to that emitted by a blackbody radiator at the same temperature, with values usually close to 1, e.g., for water ε_s = 0.97 (Robinson & Davies 1972), and for snow 0.97–1.0. The surface albedo, i.e., the capability of the surface to reflect the incoming irradiance, is a variable that varies highly temporally, spatially and spectrally from 0 to 1, depending on the surface properties. Hence, for the surface radiation balance, changes in albedo values are the most critical.

When snow melt rate is computed, all the variables affecting this heat exchange are required. Snow melt depends on the heat exchange between the snowpack and its environment. The energy balance of the snowpack can be written (Kuusisto 1984):

$$E_m = E_{SWn} + E_{LWn} + E_s + E_l + E_p + E_g - E_t \tag{2.7}$$

where E_m is the energy available for the snow melt, E_{SWn} is the net SW radiation, E_{LWn} is the net LW radiation, E_s is the sensible heat flux, E_l is the latent heat flux, E_p is the heat content of precipitation, E_g is the heat exchange at the ground surface, and E_t is the change of the internal energy of the snow-pack.

According to Kuusisto (1984), the components E_{LWn}, E_s and E_l can be considered to be limited to the snow surface or the uppermost surface layer with a thickness of a few millimeters, and E_m, E_s and E_t can be distribued throughout the snow pack. Intra-pack snowmelt can occur due to solar radiation even if the temperature of the snow surface layer is below zero. In practice snowmelt can start at the snow surface even if the temperature within the snowpack is negative, and the base of the snowpack at very low air temperatures (Kuusisto 1984).

For melting snow, the density of snow increases. Density has been used as a proxy for snow age (Doherty et al. 2016). Density refers to mass per volume, usually specified in [kg/m^3]. Snow density can be given as a ratio [%] to the water density 1000 kg/m^3.

2.3.1 Albedo of clean snow

The SZA dependency for surface albedo (U-shape) can be been expressed as (Briegleb et al. 1986):

$$\mathrm{BHR}(\cos\theta) = \mathrm{BHR}_0 \frac{(1+p)}{1+2p\cos\theta} \tag{2.8}$$

where BHR_0 is the broadband albedo for $\cos\theta = 0.5$ ($\theta = 60^o$) as given in their Table 2, and p is an empirical parameter.

Briegleb et al. (1986) measured various surfaces to determine the value of their empirical parameter p. They report $p = 0.4$ for arable land, grassland and desert, and $p = 0.1$ for all other types. According to these authors, ignoring the SZA dependence by using $\cos\theta = 0.5$ for all SZA, their model gives a 10 % variation of the TOA albedo from SZA of 0^o–60^o, compared to the observed ~30 % TOA albedo variation.

The directional reflectance properties of a target are defined by its spectral Bidirectional Reflectance Distribution Function (BRDF_λ) [sr^{-1}], which can not be directly measured (Schaepman-Strub et al. 2006). When directional reflectance properties of a surface are measured, the procedure usually follows the definition of a spectral reflectance factor BRF_λ [unitless], given by the ratio of the reflected radiant flux Φ_r [W] from the surface area to the reflected radiant flux from an ideal and diffuse surface Φ_r^{id} [W] of the same area, under identical geometry and single direction illumination (Schaepman-Strub et al. 2006):

$$\mathrm{BRF}_\lambda = \frac{\mathrm{d}\phi_r(\theta_i,\phi_i;\,\theta_r,\phi_r;\lambda)}{\mathrm{d}\phi_r^{id}\,(\theta_i,\phi_i;\lambda)} \tag{2.9}$$

where $(\theta_i,\phi_\mathrm{i})$ is the incident solar angle and $(\theta_r,\phi_\mathrm{r})$ the reflection angle (zenith, azimuth).

If the surface reflects the incident radiation isotropically, it is called a Lambertian reflector. For the ideal Lambertian surface there is no angular dependency. Both clean and dirty snow represent non-Lambertian surfaces (Peltoniemi et al. 2015). In remote sensing applications, the Lambertian assumption for snow needs to be corrected (Li et al. 2007). When an object has a sharp reflectance maximum in the backward direction, it is called a hot spot. Snow, in turn, is known as typically forward scattering (Peltoniemi et al. 2015).

The geometric manner in which the object reflects energy is also important. This factor is primarily a function of the surface roughness of the object. In specular reflectance the angle of reflection equals the angle of incidence. Rough surfaces can reflect uniformly in all directions and act as diffuse (Lambertian) reflectors. Polarized reflectance, in turn, has been considered to be generated by specular reflection at the surface of reflecting elements, such as leaves, or rocks and sand grains (e.g., Hansen and Hovenier 1974). At the top of the atmosphere, solar radiation is unpolarized, but specular reflection and atmospheric scattering generate polarized radiation.

For snow, the albedo is typically very high compared to other natural objects or surfaces. In the UV and VIS range, the albedo for clean snow is ~0.97–0.99 (Wiscombe and Warren 1980, Grenfell et al. 1994, Hudson et al. 2006). The most important factor to determine the snow albedo is the snow grain size (Wiscombe and Warren 1980, Warren and Wiscombe 1980, Mayer and Kylling 2005, Flanner et al. 2007, Gardner and Sharp 2010). Recent studies have also used the snow specific surface area (SSA) to determine the optical properties of the snow, where SSA is usually defined as the surface area per unit mass (Gallet et al. 2014).

According to the theory (Wiscombe and Warren 1980), snow albedo decreases as the grain size increases. A smaller effective radius increases the probability that an incident photon will scatter out of the snowpack (Gardner and Sharp 2010). Melting snow undergoes a metamorphism process that modifies the spectral albedo (Weller 1972). The liquid water content of snow increases, and wet snow has a lower albedo than dry snow (Blumthaler and Ambach, 1988). When snow ages, with or without melting, snow grain size increases and albedo lowers (Wiscombe and Warren 1980).

More recently, Räisänen et al. (2015) have investigated the single scattering (ω) properties of snow and developed new parametrizations for RT models. The single scattering albedo refers to the ratio of scattering efficiency to total extinction efficiency

$$\omega = \frac{\sigma s}{\sigma s + \sigma a} \tag{2.10}$$

where σs and σa are the scattering and absorption coefficient, respectively.

The single-scattering albedo is unitless, and a value of unity implies that all extinction is due to scattering (a single-scattering albedo of zero implies that all extinction is due to absorption). Räisänen et al. (2015) stated that in many radiative transfer applications single-scattering properties of snow have been based on the assumption of spherical grains due to the convenience of using Mie theory, although snow consists of non-spherical grains of various shapes and sizes. Räisänen et al. (2015) say that often the spectral

albedo of snow can be fitted by radiative transfer calculations under the assumption of spherical snow grains, when the effective snow grain size is considered an adjustable parameter (i.e. determined based on the albedo rather than microphysical measurements). In most (if not all) physically based albedo parameterizations that explicitly link the albedo to snow grain size, spherical snow grains are assumed. The new approach used angular scattering measurements of blowing snow to construct a reference phase function, i.e., the intensity of the scattered light as function of scattering angle, for snow.

The albedo of a glacier, lake or sea ice is influenced by the same factors as in case of snow, with the exception that instead of being governed by grain size, the frequency and location of scattering events (air-ice interfaces) are determined by the size and distribution of air bubbles, brine inclusions and cracks within the ice (Gardner and Sharp 2010).

2.3.2 Albedo of dirty snow

Snow containing light-absorbing impurities has a lower albedo than clean snow (Warren and Wiscombe 1980, Flanner et al. 2007, Gardner and Sharp 2010, Hadley and Kirchstetter 2012). Modeling of the dirty snow albedo is complicated by the fact that the light absorption by particles in the snow depends on the snow and impurity grain sizes and shapes.

Originally, Warren and Wiscombe (1980) stated that light-absorbing particles in snow offer an explanation for the discrepancy they found between the theory of snow albedo (Wiscombe and Warren 1980) and the observed albedo, and which could not be resolved on the basis of near-field scattering or nonsphericity effects. Warren and Wiscombe (1980) refer to the careful measurements in the Arctic and Antarctic that revealed a "grey absorber" (suggesting soot affecting these data rather than red color desert dust), whose imaginary part of the refractive index was nearly constant over the visible spectrum. The refractive index is a complex number of $m = n+i\,\kappa$, where the real part n is the refractive index and the imaginary part κ is the absorption.

Furthermore, small highly absorbing particles, present in concentrations of only 1 part per million by weight (ppmw) or less can lower the snow albedo in the visible by 5–15 % from the high values of pure snow (Warren and Wiscombe 1980).

Small amounts of strongly absorbent impurities like soot, dust and volcanic ash, lower the snow albedo in the spectral region where the absorption by ice is the weakest ($\lambda < 0.9$ μm) (Gardner and Sharp 2010). These authors further explain that at shorter wavelengths, photons generally experience more scattering events and travel a greater distance through snow, increasing the probability that the photon will encounter an absorbing impurity and not re-emerge from the snowpack. As the effective grain radius of snow increases, the average travel path lengthens, further increasing the probability of encountering an absorbing impurity. For wavelengths $\lambda > 0.9$ μm, the already strong absorption by ice leads to short travel paths, and the snow spectral albedo is negligibly influenced by the presence of impurities. Impurities located within ice grains (internal mixture) are 1.4 times more absorbing than impurities located in the air (externally mixed), but impurities concentrated near the surface have a greater impact on the albedo.

More recently, a new approach to isolate the effect of BC on snow albedo through laboratory experiments (to quantify the snow-albedo reduction associated with increasing amounts of BC and as a function of snow grain size) was developed in Hadley and Kirchstetter (2012). These authors also compared their experimental observations with the output of the Snow, Ice and Aerosol Radiation (SNICAR) model of Flanner et al. (2007), as a step towards verifying the predicted climate impacts of BC in snow. Snow was made in the laboratory with BC concentrations ranging from 0 to 1700 ppb. Their laboratory snow grains were spherical (equivalent to those of snowpacks simulated by models) and resembling naturally aged and rounded snow grains better than freshly fallen flakes. They examined different sizes of snow grains characterized by optical effective radii (R_{eff}) of 55, 65 and 110 μm.

Hadley and Kirchtetter (2012) measured decreasing snow albedo with increasing levels of BC contamination, where the radiative perturbation of BC was largest in VIS and became insignificant in NIR, confirming the fundamental assumption of a BC-induced snow-albedo reduction as hypothesized by Warren and Wiscombe (1980). The wide span in the simulated spectral albedo of BC-contaminated snow illustrated sensitivity to the mass absorption cross section (MAC) for BC. The MAC is a measure of how much sunlight BC particles can absorb, often expressed in units of m^2g^{-1} (AMAP 2015). The mass absorption cross-section MAC is the light absorption coefficient (σ_{abs}) divided by the density of the particle material multiplied with the volume of material in the particle (Adler et al. 2009):

$$\mathrm{MAC} = \frac{\sigma_{abs}}{\rho V} \tag{2.11}$$

The upper limit of their simulated spectral albedo corresponded to a BC MAC equal to 7.5 $m^2\ g^{-1}$ (at 550 nm), reasonable for freshly emitted BC. Their lower limit corresponded to snow contaminated with BC that is twice as absorbing (MAC = 15 $m^2\ g^{-1}$), and usable for atmospherically aged BC. Their results show that the albedo of both the pure and the BC-contaminated snow was lower when snow grains are larger. For example, an increase in R_{eff} from 55 to 110 μm causes a decrease of the pure-snow albedo by 0.05 (from 0.82 to 0.77), and an increase of solar absorption in snow by 28 %. Moreover, the radiative perturbation of BC in snow was amplified with increasing snow grain size (as predicted by Warren and Wiscombe 1980). Hadley and Kirchstetter (2012) conclude that their measurements supported the inclusion of a positive feedback in climate models to account for the increased solar energy absorbed by BC in ageing snow. They did not measure melt rate, but state their data to be consistent with an earlier study where enhanced snow-melt rate in BC-contaminated snow were measured.

3 Materials and methods

3.1 Radiometric measurements

Radiometric measurements of incoming and reflected solar radiation, measured with various kinds of passive instruments, are included here. Broadband (BB) radiometers measure an integrated value over a certain wavelength range, while multiband filter radiometers (MBFR) measure simultaneously several integrated wavelength ranges. Spectroradiometers, in turn, separate the radiation into small wavelength bands, with a typical resolution of 1 nm or less. Spectral measurements form the basis to which lower resolution measurements, as well as satellite and model data, can be validated and verified. Data of all these types of BB, MBFR, and spectral radiometers, at wavelengths of UV, VIS and NIR, for incoming and reflected EM radiation, were used for this thesis. It can be noted here that the operational meteorological local albedo is defined to be measured bihemispherically at a standard height of 1–2 m (WMO, 2008, I. 7).

Figure 3.1. Incoming and outgoing solar irradiance data measured by broadband (type SL-501 and CM-14), multifilterband (type NILU-UV) and spectral (type Bentham) radiometers were used in PAPER I–II.

3.1.1 Broadband UV and VIS albedo

The UV albedo measurements were the focus of PAPER I, while in PAPER II these observations were utilized together with the VIS broadband and spectral albedo data. The UV albedo data were obtained from the FMI operational albedo field in Sodankylä, FMI Arctic Research Center (FMI-ARC), to the north of the Arctic Circle. The measurements on the UV albedo of Arctic snow were started in 2007 under prof. Esko Kyrö's bipolar Arctic-Antarctic research project, with the help of FMI-ARC and the FMI Observation Unit (FMI-HAV). I put effort into initiating these measurements, which were included as part of the FMI International Polar Year (IPY 2007–2008) activities. Since 2007, the UV albedo measurements on the FMI operational albedo field have been maintained

continuous during snow time. The data are stored as 1-minute average values in the FMI Climate data base. These data have also been agreed to be included in the WMO GAW data base of the World Ozone and Ultraviolet Radiation Data Center (WOUDC), Canada.

Two UV sensors of SL501 (www.solarlight.com) with similar spectral and cosine responses (Fig. 1 in PAPER I) have been used, one facing upwards and the other downwards, at a height of 2 m from the ground. For the albedo measurements, a fixed device for the setting up and support of the two sensors, including independent leveling possibilities for the upward and downward SL501s, a blower to keep the sensors defrosted, and a data logger system, was planned and constructed at FMI-HAV.

The SL501 spectral response resembles the action spectrum for erythema, wavelengths in the UVB (280–310 nm) being most weighted (Seckmeyer et al. 2005). The erythemally weighted snow UV albedo, BHR_{ery}, is measured as the ratio of upwelling UV irradiance E_{ery} to the downwelling UV irradiance bihemispherically at 2π :

$$BHR_{ery} = \frac{Eery\uparrow}{Eery\downarrow} \tag{3.1}$$

where E_{ery} represents the bihemispherically measured temporal and spectral integral of the convolution of the solar irradiance and the erythemal response function.

The electrical signal (U) of the SL-501 sensor is related to the incoming erythemally weighted UV-B irradiance. The conversion of the raw signal into erythemal irradiance E_{ery} [W/m^2] requires a calibration factor with knowledge of the SZA and O_3 (as formulated by Webb et al. 2006):

$$E_{ery} = (U - U_{offset})\, C\, f_n(\theta, TO_3) * \varepsilon(T) * Coscor(\theta) \tag{3.2}$$

where E_{ery} is erythemal effective irradiance, U is the measured electrical signal from the radiometer, U_{offset} is the electrical offset for dark conditions, C is the calibration coefficient (a constant value determined for specific conditions like $\theta = 40^o$ and $O_3 = 300$ DU), f_n is a function of a calibration matrix normalized at solar zenith angle $\theta = 40^o$ and $O_3 = 300$ DU, $\varepsilon(T)$ is the temperature correction function, Coscor is the cosine correction function.

In practice, the temperature of the sensor is regulated (not corrected), and the calibration is made using a fixed calibration coefficient provided by the Finnish Radiation Safety Authority (STUK). The calibration procedure includes various SZA and O_3 values, but one optimized calibration coefficient value from these is calculated for each sensor. Because of the fixed sensor specific calibration coefficient value (one number per one sensor, valid for the time period following after the calibration until the next calibration), extra consideration has to be paid on the scientific usability of these data.

In our case, the sensors for upward and downward measurements are selected to represent as similar cosine and spectral responses as possible, and the sensor with the better response is used to measure the smaller signal of outgoing reflected radiation. The effect of cosine error is smaller for the upwelling reflected radiation due to the missing

direct component. Therefore under clear sky and high SZA the surface albedo derived from SL501 may be an overestimation of the real surface albedo. Uncertainties and errors decrease with increasing diffuse radiation under the full cloudiness or lower sun.

In PAPER I, an empirical calibration to the data is made, by calibrating one SL501 sensor with another one. Three SL501 were used for this purpose. The irradiance measured by the albedo sensors and one independent SL501 on the roof of the observatory were compared. Due to the SZA dependent uncertainty remaining in the data calibrated this way, the data is also divided into subsets, representative of certain SZA only.

In addition to SL501 UV sensors, field pyranometer broadband surface albedo data from the SNORTEX field campaign were included in PAPER II (Fig. 6 in PAPER II). The sensor is a Kipp & Zonen CM-14 albedometer (www.kippzonen.com) measuring at one non-weighted broadband from 310 to 2800 nm, and whose relative accuracy was estimated at 5–10 %. The general technical data of the CM-11 pyranometer applies to the CM-14 albedometer, and the relative spectral transmittance is largest (> 0.5) at 400–900 nm. The CM-14 instrument was carefully leveled on a tripod and operated without breaks during the field day. The instrument was mounted at a height of 1.5 m, implying an observed area with a radius of 15 m. During postprocessing (post-processed data provided by the co-author AR), the data were corrected for the shadowing effect of the tripod legs and imperfections in cosine response at high solar zenith angle conditions. These pyranometer data were used as an independent data set to give evidence for the measured low surface albedo values.

3.1.2 Multiband measurements on the snow surface albedo

A multichannel radiometer of type NILU-UV (www.nilu.no) was used for PAPER I to provide an independent ancillary data set. Multichannel instruments are like several wide spectral channel broadband instruments within one. The calculation of UV and VIS (or PAR channel) irradiance from the MBFR instruments may be affected, e.g., by SZA, variable ozone and cloudiness, and the fact that UV and VIS/PAR are not measured spectrally. There are at least three MBFR instruments that have been commonly used: type NILU-UV, type GUV (www.biospherical.com, applied in the US National Science Foundation (NSF) UV Radiation Monitoring Network), and type UVMFR (www.yesinc.com). Here one NILU-UV was installed looking downwards in the FMI operational surface albedo field (same place as for the SL501 albedo sensors) of the Sodankylä Arctic Research Center. Another NILU-UV was facing upwards at 30 m distance on the roof of the FMI Sodankylä Observatory.

The UV surface albedo can be calculated as a ratio of downwelling irradiance to upwelling radiation. The NILU-UV has a teflon diffuser, and the incoming radiation is passed through filters for band selection and is received by 5 or 6 silicon detectors placed side by side underneath the diffuser. The total (diffuse and direct) incoming UV irradiance is measured in five channels with center wavelengths at 305 nm, 312 nm, 320 nm, 340 nm, and 380 nm. Each channel bandwidth is about 10 nm. The sixth channel covers the photosynthetically active radiation (PAR, 400–700 nm). A portable lamp unit for relative calibration can be used to check the relative stability. The erythemal irradiance E_{ery} is

calculated using a linear combination of the five channels of the instrument, and utilizing the absolute calibration coefficients (provided by the NILU Corp.):

$$E_{ery} = a(v1) + b(v2) + c(v3) + d(v4) + e(v5) \quad (3.3)$$

where a,b,c,d and e are the absolute calibration coefficients for the raw voltage signal (vi) of each of the five channels of the instrument.

3.1.3 Spectral snow surface albedo

In addition to the SL-501 UV, pyranometer, and multiband-filterradiometer (MBFR) NILU-UV data, Bentham spectrometer data were used for investigating the snow surface albedo in PAPER II. Guidelines for the spectral instruments are found in the WMO GAW report No. 125 and 212 (WMO 2001 and 2014). In practice, the measured specral irradiance $E_M(\lambda)$ varies from the "true" spectral irradiance $E(\lambda)$ due to various errors which may be related with the instrumental characteristics, like the calibration procedures, or the operational procedures.

Due to its big size and weight Bemtham suits best for measuring the surface albedo in one location, as done here. Instrumentation for spectral surface albedo measurement has been improved recently, and good-quality portable field spectrometers with large spectral ranges (300–2500 nm) are available. Here, the Bentham spectrometer was operated by an experienced Bentham specialist (the co-author SK), who provided the corrected data used in PAPER II.

3.2 Snow analysis and measurements

3.2.1 BC/OC in snow

Results of the analysis of BC/OC in snow in Sodankylä are utilized in PAPER II and PAPER III. Snow surface (appr. first 2 cm of snow) samples have been collected during snow covered season from the same location, protected with reindeer fences, in the Sodankylä Arctic Research Center for impurity analysis on a weekly basis since 2009. The sampling has been made by a FMI-ARC technician. Snow BC/OC samples have first been collected and filtered, and then the filters have been sent for analysis to University of Stockholm, Sweden (Prof. Johan Ström). These BC/OC results had not been investigated or published until PAPER II, where BC/OC data of 2009–2011 are utilisized to understand the measured and modeled snow surface albedo. BC results were also used in PAPER II for the long-range transport analysis to study the origin of the BC in snow. For PAPER III, all FMI snow BC/OC analysis data available with simultaneous snow density data were utilized. These consisted mainly of campaign data.

The sampling and analysis for BC/OC in snow follow the general methodology developed by Forsstrøm et al. (2009) and Aamaas et al. (2011). Surface snow is collected in a container, then carefully melted in a microwave oven (avoiding evaporation and increased impurity concentration), and filtered through sterilized micro-quartz filters (55 mm diameter) using a pump attached to the filtering system to create a vacuum during filtering. The volume of meltwater is needed for concentration conversions. Dried filters are analyzed with a Thermal/Optical Carbon Aerosol Analyzer (OC/EC) (Sunset Laboratory Inc., Forest Grove, USA) for their elemental carbon (EC) and organic carbon (OC) concentration, following the NIOSH 5040 protocol developed by Birch (2003). The EC is used as a proxy of BC. The thermal–optical method was created by Birch and Cary (1996), where a detailed description of the method is presented. In practice, a piece of the filter (1 cm^2) is punched for the analysis. The thermal-optical carbon aerosol analyzer first heats the filter piece in a helium atmosphere, and organic carbon released from the filter is detected. Then, the filter is heated in an oxygen atmosphere, and EC is released and detected.

For PAPER III, I collected and filtered snow samples within SNORTEX-2010 experiments, using the methods of Prof. Steven Warren (Doherty et al. 2010). Samples were collected to allow a later method comparison between the spectrometer and the Single Particle Soot Photometer (SP2) analysis methods. These filters were sent for analysis to the University of Washington, USA, and analysed by Dr. Sarah Doherty using a spectrometer method, and the duplex samples were stored in a freezer to wait for the SP2 method development.

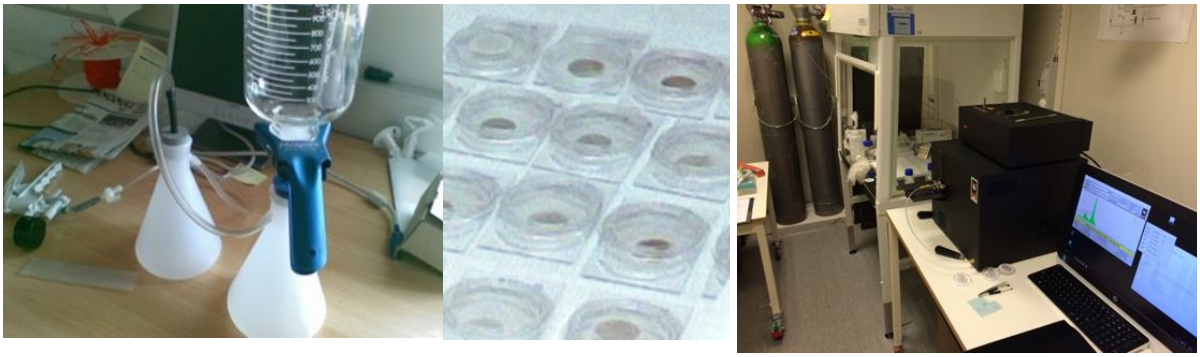

Figure 3.2. Snow EC/OC analysis data are used for PAPER II–III. The collected snow samples are first filtered, then the filters are analyzed using the NIOSH thermo-optical method. The photo on the right shows the EC/OC analyzer currently at FMI. Photos O. Meinander.

3.2.2 Snow density

For PAPER III, snow densities (weight per volume) were measured manually, for either the whole snowpack vertical column (snow tube and balance for SR and SNORTEX experiments), or for separate horizontal snow layers (density cutter and a balance for the SoS experiment to measure the density of the visually dirty surface snow). Combined data

of snow density and BC were collected from all existing Sodankylä campaigns for PAPER III. The hypothesis of snow density effects of impurities existed before any data. After the first promising results were obtained, all possible combined FMI data of density and BC were collected together. The uncertainties related to the BC and density measurements are considered in PAPER III.

3.2.3 Snow fork for snow liquid water content

PAPER II uses the measurements of snow liquid content with the commercially available Snow Fork by Toikka Oy (www.toikkaoy.com). The sensor is a steel fork that is used as a microwave resonator. The Snow Fork measures the electrical parameters of resonant frequency, attenuation, and 3 dB bandwidth. The liquid water content is calculated from these measurements. In addition to the actual snow liquid water content, the snow impurities and grain sizes, hardness and density, etc., may affect the measurement results. As the calculation is based on semi-empirical equations of natural clean snow, the calculation is expected to contain more uncertainties in case of dirty snow.

3.2.4 Meteorological Automatic Weather Station data

The Sodankylä automatic weather station (AWS) measures the state of the atmosphere at a height of 2 m once a minute. From these data, information on, e.g., air temperature, the onset of precipitation, snow depth and cloud cover, can be obtained. The Sodankylä Arctic Research Center measurement program includes a large variety of environmental parameters. Here use was made of the daily minimum and maximum air temperatures and snow depth for PAPER I. In PAPER II, the measured aerosol parameters and total ozone as input values for the RT calculations, and the beginning and amount of rain for SILAM transport model calculations.

3.2.5 Snow grain size and other snow properties

In PAPER I–II, snow grain size is visually estimated using a plate with two grid sizes of 1 mm and 2 mm (Fig. 4 in PAPER I). Snow grain size data were utilized for the surface albedo data analysis in PAPER I. The snow grain size and shape data (provided by the co-author AK) was based on Fierz et al. (2009) for seasonal snow on the ground.

A simple “Snow ball test” is used for PAPER II. The test is in regular use in all Sodankylä snow research. This practical test tells if the properties of snow are such that one succeeds in making a snowball out of the snow on the ground. Snowballs can only be made when snow properties are suitable for making them, i.e., when snow contains water but is not too wet. With the test, for instance the start of snowmelt can be easily detected, as corresponding snow property information would be hard to determine otherwise.

Additional ancillary data of snow grain shape, snow layer thicknesses, and snow temperature are available for PAPER I–II as part of the SNORTEX. Although some of the

data allow investigation of the properties of the snowpack, the focus of the original papers and the thesis summary is on surface snow (not on snowpack properties).

3.2.6 BC and volcanic particles used in the experiments

For the Soot on Snow (SoS) experiment at Sodankylä (PAPER III), BC (soot) and Icelandic volcanic ash and silt particles (Fig. 3.3) were collected. Soot originated from chimneys of residential wood-burning fireplaces, except for one experimental spot with soot from a chimney of an oil burner, and another one with soot from a peat-burning power plant. Volcanic sand in PAPER III was collected from Myrdalssandur, Iceland. The sand was a dark mixture of the volcanic ash of glaciofluvial nature, originating from under the Myrdalsjokull glacier, which may be mixed with the ash of the Eyjafjallajokull eruption in 2010 and the Grimsvotn eruption in 2011. The glaciogenic silt was collected close to the Myrdalssandur and it was lighter in colour than sand, from light-brown to slightly yellowish colour consisting mainly of silt and some coarse clay sized particles, which could be deposited on the local glaciers as well as transported over several hundreds of kilometers towards Europe. These particles were collected from ground as such and were not sieved nor cleaned before the experimental utilization.

For PAPER IV, different Icelandic ash and dust particles were utilized. Icelandic volcanic ash was collected on Eyjafjällajökull just after the eruption ended in late May 2010 (Fig. 1 of PAPER IV). The ash particles were sieved and the grains with sizes 1 ϕ (500 μm) and 3.5 ϕ (90 μm) were used in the experiments in FMI Kumpula. In addition, both particle types were investigated by Scanning Electron Microcopy SEM analysis for their shape, size and surface features. The bulk density for 1 ϕ ash was 2.7 g/cm^3 and for 3.5 ϕ it was 2.5 g/cm^3. The Krumbein phi (ϕ) scale for particle size is defined as:

$$\phi = -log_2 D/D_0 \qquad (3.4)$$

where D is the diameter of the particle, D_0 is a reference diameter (equal to 1 mm to make the equation dimensionally consistent).

Icelandic dust samples were collected by collecting snow samples at 16 locations on the surface of Vatnajökull in October 2013. The samples represent dust that was deposited on the glacier surface during one summer. The top 8 cm of the snow surface (about 1–2 kg of snow) was collected from an area of appr. 57 x 10^{-3} m^2. The samples were then melted, evaporated and the mass of the dust was weighted. This information was then used to link the experimental results of PAPER IV to natural conditions in Iceland.

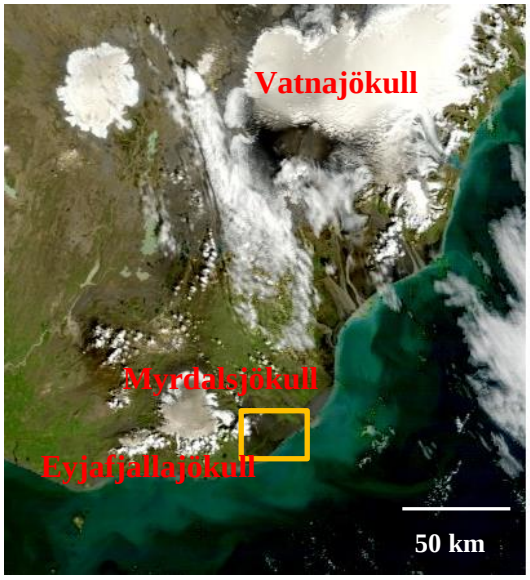

Figure 3.3. The Terra/MODIS satellite image (downloaded from NASA LAADS Web) of Iceland shows the origin of the collected volcanic material from Myrdalsjökull glacier (the yellow rectangle on the southern coast). The origin of volcanic ash mixed with the particles was from volcanoes of the Eyjafjallajökull (west from Myrdalsjökull) and Grimsvötn (under Vatnajökull glacier on the eastern coast). Icelandic dust–cryosphere interaction is a topic included in PAPER III–V. Image courtesy of NASA Level-1 and Atmosphere Archive & Distribution System (LAADS) Distributed Active Archive Center (DAAC), Goddard Space Flight Center, Greenbelt, MD.

3.3 Experiments

Experiments were an essential part of the work included in the original publications of this thesis. Two large-scale experiments were arranged in Sodankylä (67°22’N, 26°39’E, 179 m a.s.l.), Finnish Meteorological - Arctic Research Center (FMI-ARC), which is part of the Pallas/Sodankylä Global Atmospheric Watch (GAW) station of the World Meteorological Organization (WMO). PAPER II is based on results gained during the SNORTEX experiment in Sodankylä (section 3.3.1). Paper IV uses Sodankylä results from SoS experiments (section 3.3.2), as well as from the SnowRadiance (SR), an ESA-funded project aiming at determining snow properties from optical satellite measurements. PAPER IV is based on results gained during indoor and outdoor experiments (section 3.3.3) carried out at FMI HQ at Kumpula Campus, Helsinki, close to the SMEAR III station (Järvi et al. 2009), i.e., Station for Measuring Ecosystem-Atmosphere relations.

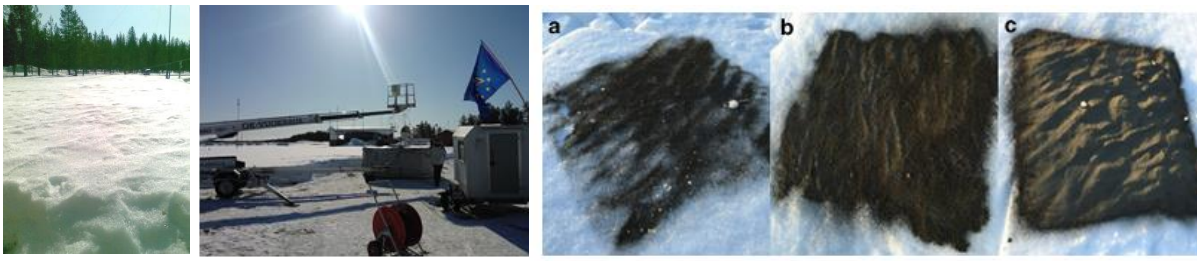

Figure 3.4. The outdoor and indoor experiments were an essential part for PAPER I–IV. SNORTEX (left) and Soot on Snow (middle) Experiments in the Sodankylä Arctic Research Center (67°22'N, 26°39'E, 179 m a.s.l.), North of the Arctic Circle (Photos O.Meinander). Icelandic ash and dust (right; a,b,c) on snow at Kumpula, closeby the SMEAR III station (60°12'N, 24°58'E), picture from **PAPER IV**. © Author(s) 2016, published with open access at Springerlink.com.

3.3.1 SNORTEX

PAPER II is an outcome of the Finnish-French "Snow Reflectance Transition Experiment" (SNORTEX, 2008–2010). SNORTEX aimed at acquiring in situ measurements of snow and forest properties in support of the development of modeling tools, and validating coarse resolution satellite products (Manninen and Roujean 2014). The SNORTEX study area was located in Finnish Lapland beyond the Arctic Circle, and benefitted from existing facilities provided by FMI-ARC. SNORTEX sites consisted of: (1) The Arctic Center at Sodankylä; with temporal daily data series of various parameters collected within SNORTEX, as well as operationally by FMI. (2) SNORTEX experiment sites in the Sodankyla region, representing different types of environment, e.g., open area, forested area, and snow on the lake.

3.3.2 Soot on Snow

PAPER III is based on The Soot on the Snow (SoS-2013) experiment. SoS-2013 was carried out in Sodankylä to study the effects of deposition of BC, Icelandic volcanic sand and glaciogenic silt on the surface albedo, snow properties and melt of the seasonal snow. The experimental area was a large, flat, fenced open space of Sodankylä airport (not in active use), and the gravel ground was not covered with concrete or asphalt. Different amounts of impurities were deposited to snow on different spots with the help of a blower and a tent. Each spot had a diameter of 4 m. Thereafter the spots were monitored until the snow had completely melted. The sites were left to develop naturally, introducing as little disturbance as possible. In addition to PAPER III, the experiment is described in Peltoniemi et al. (2015) and Svensson et al. (2016) (where I am a co-author).

3.3.3 Icelandic dust

For PAPER IV, four outdoor and laboratory experiments were carried out using three setups of: 1. snow (AoS-2015); 2. ice (AoI-2015, Roof 2015); and 3. snow over ice (AiC-2015). Ash of 1 ϕ grain size was used for the AoS-2015, AoI-2015 and AiC-2015 experiments, whereas ash of 1 and 3.5 ϕ was used for the Roof 2015 experiment. Layer thicknesses were measured in dry condition of the ash.

The Ash on Snow (AoS-2015) experiment was an outdoor experiment on the effect of ash on snow in natural conditions in an urban area in Kumpula Campus area closeby the SMEAR III station, in Helsinki. The experiments started on 6 February 2015 using natural snow in a fenced area, i.e., unperturbed by direct human interference. Three different amounts of ash (15 g (166 g m^{-2}); 85 g (944 g m^{-2}); and 425 g (4722 g m^{-2}, 15 mm layer thickness)) with grain size 1 ϕ, were deposited on an area of 0.3×0.3 m^2 on a snow surface. Snow density was 280 kgm^{-3}. Snow depth and temperature were then monitored for 17 days when the snow melted naturally.

A controlled experiment with ash on ice was made both indoors (AoI-2015) and outdoors (Roof-2015), to identify and separate the effects of temperature and solar irradiance. Ash on Ice (AoI-2015) were laboratory experiments to examine the effect of ash layer thickness on ice melting, in a temperature-stabilized environment kept at +24°C. For these experiments, small, transparent plastic boxes were filled with 200 ml of tap water and frozen (surface area 84 cm^2). This resulted in an ice layer with a depth of 25–28 mm. To find the insulating threshold of ash on ice, four different amounts of the 1 ϕ impurity were deposited (3 g (1.3 ml, 366 g m^{-2}), 35 g (15 ml, 4219 g m^{-2}, 1 mm layer thickness), 71 g (30 ml, 8437 g m^{-2}, 3 mm layer thickness) and 283 g (120 ml, 33,749 g m^{-2}, 9–13-mm layer thickness)). After deposition of material, the ice was transferred into white pots with holes in the bottom to measure the meltwater runoff.

The laboratory experiments were repeated outside on the roof of the FMI building in sunny conditions to study effects of solar irradiance in addition to that of temperature above zero. The experiment was repeated with the same volume of impurities, but using two different grain sizes of the Eyjafjallajökull 2010 ash: 1 ϕ (samples A) and 3.5 ϕ (samples B). The concentrations for the 3.5 ϕ B-samples were: 2.46 g (1 ml, 292g m^{-2}); 36.8 g (15 ml, 4385 g m^{-2}, 1 mm layer thickness), 73.7 g (30 ml, 3–5-mm layer thickness, 8772 g m^{-2}) and 294.7 g (120 ml, 35,086 g m^{-2}, 9–13-mm layer thickness). The concentrations for the 1 ϕ ash were the same as used in AoI-2015.

The Ash in Container (AiC) experiment was performed in a cold container of the University of Helsinki snow laboratory, where ash was deposited on snow over ice. The purpose was to investigate how ash insulates and prevents snow melt compared to the outdoor results. The AiC setup was closer to the conditions on the glacier surface, than the ash on snow setup. A big pot, inside a cold container, was filled at the bottom with a thick ice layer and on top of that an 8.5 cm thick layer of snow was added. Two different amounts of impurities were used (the same as in the outdoor experiments): 15 g (166 g m^{-2}) and 425 g (4722 g m^{-2}, 15 mm thickness) of 1 ϕ Eyjafjallajökull ash on a 0.3×0.3 m^2 area. The experiment started at a temperature of −10°C inside the container; then, the cooling system was shut down, and the laboratory adapted to outdoor temperatures up to +4°C. Snow depth and behavior of the ash were monitored.

3.4 Modeling

For the thesis, results from three different types of models were utilized. These include the RT modeling (section 3.4.1), snow surface albedo modeling (section 3.4.2), and long-range transport modeling (section 3.4.3). The RT modeling was needed to show how big error the observed SZA surface albedo asymmetry would cause on the satellite based detection of the surface albedo when the SZA asymmetry is not corrected. The surface albedo modeling was used to investigate if and how the measured surface albedo values could be simulated. Snowpack or snow melt modeling were out of the scope of the current work. Transport modeling results were needed to investigate what could be the source for the unexpectedly high BC concentrations measured in Sodankylä seasonal surface snow.

3.4.1 RT modeling

The RT model LibRadtran (Mayer and Kylling 2005) was utilized for irradiance estimates in PAPER II. For the physical modeling of the solar irradiance, there are several RT models available. These include the Library for radiative transfer LibRadtran (www.libradtran.org); FastRT (http://nadir.nilu.no/~olaeng/fastrt/fastrt.html with a simpler version in http://nadir.nilu.no/~olaeng/fastrt/fastrt-ez.html); the Tropospheric Ultraviolet and Visible (TUV) Radiation Model of the National Center for Atmospheric Research (NCAR, USA); the Santa Barbara DISORT Atmospheric Radiative Transfer (SBDART, http://www.crseo.ucsb.edu/esrg/pauls_dir/); and the SMARTS2 (e.g., http://www.fsec.ucf.edu/en/publications/pdf/FSEC-PF-270-95.pdf). In the model, a radiative transfer equation solver is needed. There are different solvers available, including 1-D and 3-D solvers. Several input parameters are required for the model inputs. These are, e.g., the Extraterrestrial Source Spectra (for which several models exist, rredc.nrel.gov), and standard atmosphere model (providing with vertical profiles of pressure, temperature, water vapor and ozone density and other gases for various climatic conditions like tropical, midlatitude summer, midlatitude winter, subarctic summer, or subarctic winter). Inputs also include a cloud model (the computation of radiative transfer within a cloudy atmosphere requires knowledge of the scattering efficiency, the single scattering albedo, which is the probability that a extinction event scatters rather than absorbs a photon, and the asymmetry factor, which indicates the strength of forward scattering), as well as aerosol models (e.g., the aerosol model by Shettle 1989) and surface models to parameterize the spectral reflectivity of various surface types like ocean water, lake water, vegetation, snow and sand; the spectral reflectivity of a large variety of surface conditions can be approximated by combinations of these basic types.

An action spectrum describes the relative effectiveness of energy at different wavelengths in producing a particular biological response. The response may refer to effects, e.g., at a molecular level (e.g., DNA damage), or at a whole organism level (plant growth). There are several UV action spectra: the erythemal action spectrum given by McKinlay and Diffey (1987), and the DNA damage action spectrum of Setlow (1974), to name a few. By multiplying the erythemal irradiance [W/m^2] by 40, UV-Index scale is gained. Often there is decline in relative response as the wavelength increases indicating

the importance of the UV-B. These responses could be more sensitive to ozone depletion, as especially UV-B irradiance increases with lower ozone levels. With a strong UV-A dependence, the ozone depletion would not have as great an impact. Radiation amplification factors (RAF) give the increase of biologically effective irradiance in response to ozone depletion. Biological weighting functions which are heavily weighted in the UV-B region (e.g., DNA) have RAF > 1, and biological weighting functions weighted outside the UV-B region, like UV-A spectral region, have RAF < 1.

3.4.2 Snow albedo modeling

In PAPER III, the Snow, Ice, and Aerosol Radiation (SNICAR) on-line version (Flanner et al. 2007) was used to obtain simulated data on the snow albedo to compare with the in situ surface albedo data. The measured parameter values of snow depth, snow grain size and elemental carbon (BC) content were used as input values to simulate a clear sky case (day 22 April) and a diffuse sky case (24 April). In SNICAR-online, there are two types of black carbon input parameters: (1) uncoated (mimicking hydrophobic particles), with properties tuned to achieve a mass absorption cross-section of 7.5 m^2g^{-1} at 550 nm (Bond and Bergstrom 2006); and (2) sulfate-coated black carbon (mimicking hydrophilic black carbon), which is composed of a weakly-absorbing shell (sulfate) surrounding BC, resulting in an absorption enhancement (per unit mass of black carbon) of about 1.5 (Bond et al. 2006). Most of the BC in the snow at Sodankylä can be assumed to originate from long-range transport, and therefore the BC in snow can be assumed to become hydrophilic. Yet, with the current snow analysis data we cannot determine that all BC would be hydrophilic. Therefore, in the simulated data, I used both these options separately to compare their effect on the surface albedo. For melting seasonal snow in northern Finland, the averaged snow density values of 329 kg m^{-3} for forest, and 349 kg m^{-3} for open sites, have been reported (Kuusisto 1984). From these the value reported for northern Finland was used. The snow BC concentration can be assumed to be approx. double the EC concentration determined by the thermos-optical method (Chow et al. 2001, Aamaas et al. 2011). The parameter value of the mass absorption coefficient MAC was tuned to produce surface albedo values close to the lowest measured surface albedo of 0.4–0.5 at UV.

3.4.3 Long-range transport modeling

The origin of the detected BC in Sodankylä surface snow samples was investigated in PAPER III by means of transport modeling. The two most commonly applied models to consider were NOAA's HYSPLIT model (REF, http://ready.arl.noaa.gov/HYSPLIT.php) and FMI's SILAM model (Sofiev et al. 2008 and http://silam.fmi.fi). SILAM was tested and found applicable for the purpose. SILAM model calculations were provided by SILAM specialists Dr. RK and MS, co-authors of PAPER III.

For the application of PAPER II, a simple method ("algorithm") was developed to study the origin of BC in snow samples using SILAM transport model calculations (Figure

3.5). First, the measured BC in snow concentrations were divided into two groups of "clean" and "dirty" cases by the day and BC contents. Snow was considered clean if it contained < 20 ppb BC, based on results by Doherty et al. (2010), and dirty if > 30 ppb. Only cases where there was snowfall before 24 h or less prior to the snow sampling were included. The modeling was then performed with SILAM (System for Integrated modeLing of Atmospheric coMposition) version v5.2. The meteorological fields from short-term operational forecasts of the European Centre for Medium-range Weather forecasts (ECMWF) were used as a driver for SILAM. The adjoint simulations were performed with resolution 0.5 × 0.25 degree on a domain 10–60 °E, 55–75 °N with 8 vertical layers of thickness from 30 m at surface to 2000 m, within a height range from surface to 6 km. The footprints were taken for the layer 150–300 m, which were expected to correspond to the height of industrial emissions due to combustion. The observational function of atmospheric concentrations corresponding to measured in-snow concentrations was taken to be uniform with height from the surface to the bottom of a cloud and weighted by snowfall intensity in time, so total sensitivity is unity. The footprints were calculated for each sample separately.

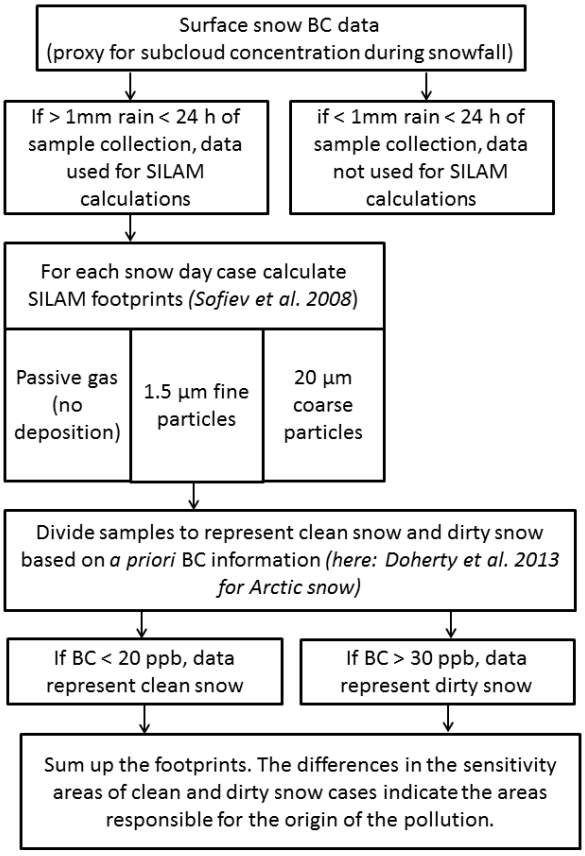

Figure 3.5. An illustration of the algorithm used to investigate the origin of the BC content in surface snow, based on text presented in **PAPER II**.

To minimize the effect of dry deposition and to ensure the consistency between observed and modeled snowfalls, only the cases were selected when snowfall was reported by both the weather station at Sodankylä and the meteorological driver, reporting more than 1 mm snowfall within 24 h before the sample collection and the amount of the precipitation agreeing within a factor of 2 between them. The volumetric content of black carbon was used as a tracer of anthropogenic pollution. With the above criteria, out of 70 snow samples we selected 10 “clean” (< 20 ppb of BC) and 12 “dirty” (> 30 ppb of BC) samples and calculated the average footprint for both classes. Since the size of airborne black carbon is unknown, the footprints were calculated for passive gas with no deposition, for 1.5 μm (fine) particles and for 20 μm (coarse) particles.

4 Overview of results and discussion

4.1 Albedo of seasonally melting snow, north of the Arctic Circle

The role of snow albedo-feedback mechanisms in snow melt is often cited as the main contributor to the Arctic climate change amplification. In Finland, Arctic snow melt related studies on the naturally layered snow have the advantage of seasonal snow melt, despite the northern location. PAPER I investigates the Arctic snow albedo and seasonal snow melt in Sodankylä utilizing both meteorological and cryospheric parameters, such as snow depth, snow grain size, and air temperature. PAPER II proceeds further and utilizes also data on light-absorbing impurities deposited in snow.

In PAPER I, a SZA-dependency (U-shape), as described in Briegleb et al. (1985), in the surface albedo data is evident (Fig. 4.1). It is explained to be possibly partly due to changed spectral response of the sensors. On the basis of the post-calibration measurements, it was calculated that for SZA of 56–60 degrees, the sensor SZA dependency (the U-shape due to difference in the spectral responses of the sensors), caused an error of less than 3 %. PAPER I states that the U-shape might be partly due to the different radiation components the upward and downward radiometers detect; for the downward looking sensor the diffuse and specular reflectance, while for the upward sensor the direct and diffuse radiation. The surface albedo data in PAPER I are then grouped according to cloudiness, as well as according to the status of accumulating or melting snow. For clear sky and fully cloudy days, a diurnal variability in the snow UVB surface albedo is found, possibly indicating changes in the physical properties of snow. PAPER I explains that if this diurnal variation in the surface albedo is due to any shadowing effects, rather than changes in the snow properties, shadowing would be best seen under clear sky conditions, and not in cloudy situations. Since this is not the case, an explanation is searched from changes in snow properties, especially snow grain melt metamorphism (change in snow grain shape and structure), and changes in the liquid water content of the snow. In addition to the U-shape and temporary diurnal variability in the surface albedo, a possible SZA asymmetry in the surface albedo is suggested in some of the data. SZA asymmetry is not studied further in PAPER I, but has been a subject included in PAPER II.

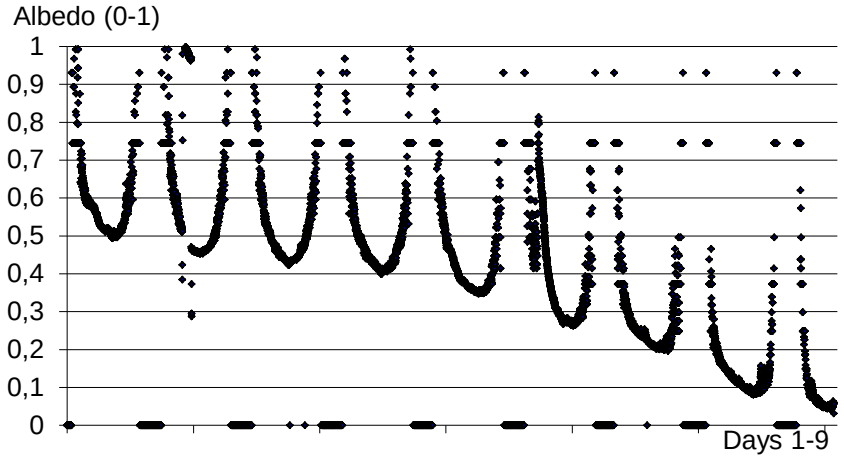

Figure 4.1. The albedo of melting snow shows the diurnal SZA dependency (U-shape, as described in Briegleb et al. 1985), and the temporal decrease in the midday albedo value. The U shape of the albedo is explained to be partly due to differences in spectral responses of the sensors, and partly due to the different radiation components the upward and downward radiometers detect: downward looking sensor detects the diffuse and specular components, while the upward sensor detects the direct and diffuser. The SL501 BRF_{ery} data are for 1-9 May (days 121-129) for SZA > 85^{o}. Redrawn based on Figure 10 of **PAPER I**.

For snow melt, the empirical results of PAPER I from Sodankylä indicate that the change of daily maximum air temperatures from below zero to above zero degrees Celsius is not enough to start the snow melt (on the basis of AWS snow height data). This is explained to indicate the importance of solar irradiance as the starting force for the snow melt. Monotonical snow height decline starts in these data one month later (day 102) than the change of maximum temperature to be above zero degrees Celsius (day 66). It can be noted here that the albedo is possible to decline with and without snow melt as a result of snow metamorphosis and evaporation.

The snow grain size is the key snow property which determines the snow albedo. Yet it is a parameter whose values are among the hardest to obtain. Snow height measurement, on the other hand, are most often available. PAPER I studies whether it is possible to express the grain size in a simple way, with the help of other environmental parameters For the case of seasonally melting snow in Sodankylä, a linear relationship is found for snow grain size as a function of the day of the year, daily maximum air temperature at a height of 2 m, and the height of the snowpack (Eq. 3 of PAPER I).

PAPER II finds diurnal asymmetry in the snow albedo (Fig. 3 and Fig. 6 in PAPER II). This means that instead of the U-shape reported in PAPER I, the albedo signal of intensively melting snow has a feature of a declining line. During each day the albedo decreases on average by 10 %. The albedo is higher in the morning than in the afternoon, i.e., the albedo is asymmetric to SZA. The measurements are made towards the Sun on a relatively flat snow surface, where the forward scattering nature of snow is detected. The diurnally declining albedo has been previously reported in Pirazzini (2004) and Wuttke et al. (2006) using broadband data. The diurnal SZA asymmetry in surface means that the

albedo decline dominates over the SZA-dependent albedo signal. The main driver of the measured albedo is therefore the intensively melting snow. The spectral change in the measured data was greater the shorter the wavelength. This is consistent with the theoretical results of Warren and Wiscombe (1980), which show that the absorption due to impurities in snow increases with the decreasing wavelength.

4.2 Effects of BC/OC on snow albedo, melt and density

Snow containing light-absorbing impurities has a lower albedo than clean snow, and this can affect snow melt via the albedo-feedback mechanism. In PAPER II–V, the snow albedo, melt and density are investigated and discussed in connection to light-absorbing impurities in snow, and BC/OC is included in PAPER II–III.

In PAPER II, the BC contents (Figure 4.2) of the surface snow layer at the Sodankylä Arctic Research Center, Finland, are found to be higher than expected based on literature, and also to increase in spring time (Table 3 of PAPER II). This increase in spring is suggested to be due to accumulation of hydrophobic BC in the surface snow during snow melt, although some of the high BC concentrations are anthropogenic soot from the Kola Peninsula, Russia (more in section 4.4). The origin of OC can be anthropogenic or natural. PAPER II says that at the time of publishing the paper in 2013, the scientific understanding of the snow organic carbon absorption has only started to develop recently. The Sodankylä results from years 2009–2011 suggest some increase of OC in snow toward the late spring (many days with > 2000 ppb in April).

The albedo of natural seasonal snow surface measured in Sodankylä, is found ~0.5–0.7 which is lower than the expected values of ~ 0.97–0.99 for clean snow (Grenfell et al. 1994, Hudson et al. 2006). In PAPER II, the solar UV and VIS albedo values in the range of 0.6–0.8 in the accumulation period, and from 0.5 to 0.7 during melting, are reported. Three independent data sets are used to confirm these observations. The low albedo values are explained to be due to large snow grain sizes of up to ~3 mm in diameter, and meltwater surrounding the grains and increasing the effective grain size, and absorption caused by impurities in snow (87 ppb BC and 2894 ppb OC). This case is further studied with the help of the SNICAR model (Section 4.4).

In addition to the snow-albedo feedback mechanism, a new hypothesis on the snow density effects is suggested in PAPER III. The paper hypothesizes that BC may decrease the liquid water retention capacity of melting snow. PAPER III also presents the first data, where both the snow density and elemental carbon content are measured (Figure 4.3). In an additional laboratory experiment, artificially added light-absorbing impurities cause a decrease in the density of seasonally melting natural snow. No relationship is found in case of natural non-melting snow. Additional laboratory experiments confirm that snow containing impurities releases melt water quicker than cleaner snow. PAPER III suggests three possible processes that might lead to lower snow density. These are: A semi-direct effect of absorbing impurities, where absorbing impurities would cause melt and/or evaporation from the liquid phase and sublimation from the solid phase of the surrounding snow, resulting in air pockets around the impurities, and thus lower snow density; or BC

effect on the adhesion between liquid water and snow grains, where BC reduces adhesion, and the liquid-water holding capacity decreases; or BC effect on the snow grain size, where absorbing impurities increase the melting and metamorphosis processes, resulting in larger snow grains, which lower the water retention capacity.

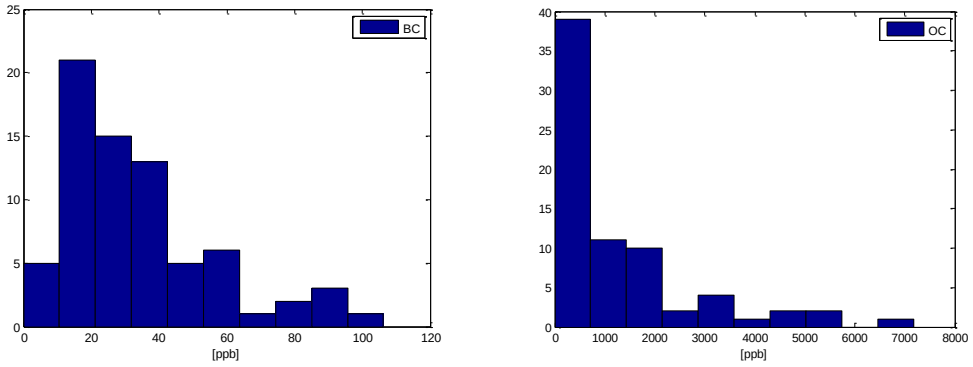

Figure 4.2. Histograms of the BC and OC concentrations [ppb] in the surface snow in Sodankylä during snow time, since the beginning of 2009 until the snow melt in spring 2011. The histograms are based on data presented in Table 3 of **PAPER II**.

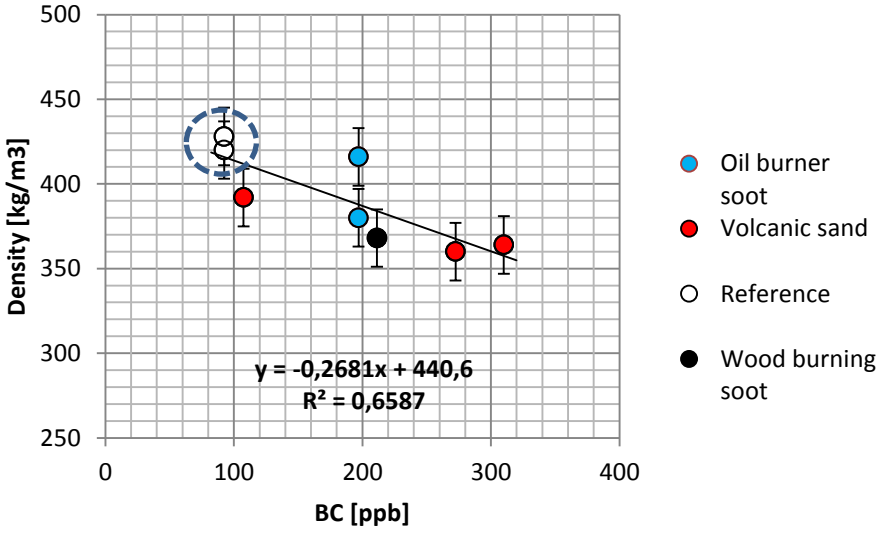

Figure 4.3. The BC content [ppb] vs density [kgm^{-3}] for the naturally melting snow in Sodankylä with and without artificially added impurities. The line is a least square fit through all the points. Redrawn on the basis of Figure 2 of **PAPER III.** © Author(s) 2014. CC Attribution 3.0 License.

4.3 Icelandic dust and cryosphere

In the Arctic region, Iceland is an important source of dust due to glacio-fluvial processes and ash production from volcanic eruptions, combined with frequent high winds. Dust is resuspended from the surface into the atmosphere in dust storms. Iceland faces 135 dust days each year (Arnalds et al. 2016). Icelandic dust and ash particles are dark in color, and due to their light-absorbing properties their impact on the cryosphere can be significant. More scientific results are needed to assess the cryospheric effects of Icelandic dust and ash.

In this thesis, PAPER IV–V deal with effects of Icelandic dust. PAPER III on BC density effects uses also data where Icelandic volcanic particles are artificially deposited in snow. However, PAPER III says that volcanic sand is assumed not to contain BC. The paper refers to Dadic et al. (2013, their Fig. 12a), and FMI's own EC analysis of volcanic sand samples with the thermal–optical method showing hardly any EC.

PAPER IV investigates the melt and insulation effects of Icelandic dust and ash on snow and ice. During volcanic eruptions and dust storms, material is deposited on the glaciers where it influences their energy balance. In PAPER IV, the effects of deposited volcanic ash on ice and snow melt are examined using laboratory and outdoor experiments. These experiments were made in Kumpula, Helsinki, during the snow melt period. Two different ash grain sizes (1 ϕ and 3.5 ϕ) from the Eyjafjallajökull 2010 eruption, collected on the glacier, are used. Different amounts of ash are deposited on snow or ice, after which the snow properties and melt are measured. The results show that a thin ash layer increases the snow and ice melt but an ash layer exceeding a certain critical thickness caused insulation (Table 4.1). The experimental results will be useful for investigating the possible consequences in the natural environment.

Table 4.1. Effective and critical thicknesses for different materials such as tephra, rock debris and dust. The effective thickness is the thickness when the material covered ablation is maximized. According to Brock et al. (2007), the critical thickness is the thickness of the material covering the ice or snow where the ablation rate of the material-covered ice or snow equals that of the clean snow or ice; more material will start to insulate. The results of PAPER IV are in italics. Reproduction of Table 1 of **PAPER IV**. © Author(s) 2016, published with open access at Springerlink.com.

Material	Effective thickness [mm]	Critical thickness [mm]
Mt St Helens (1980) ash	3	24
Hekla (1947) tephra	2	5.5
Rock debris	~10	~15–50
Villarrica tephra	-	< 5
Dust (largely organic matter)	-	1.33
Eyjafjällajökull ash (2010, 1 ϕ)	*1*	*9–15*
Eyjafjällajökull ash (2010, 3.5 ϕ)	*≤ 1–2*	*13*

In PAPER V, the cryospheric role of Icelandic dust is discussed and hypothesized. PAPER V refers first to Benning et al. (2014), where microorganisms, such as the pigmented algae that reside in snow and ice, are argued to possibly cause a substantial reduction in the albedo. Thereafter Dumont et al. (2014) is cited, where the springtime darkening of the Greenland Ice Sheet (GrIS) (observed since 2009) is suggested to be due to an increased load of light-absorbing impurities in snow that consist of soot or dust and, potentially, microorganisms. Tedesco et al. (2015) provide arguments on the reduction of the albedo by cryoconite (a mixture of dust, pebbles, soot, and microbes). The old work of the Finnish explorer Adolf Erik Nordenskiöld (1883) is brought up. Contradiction to these is presented by work on the influence of satellite sensor degradation (Polashenski et al. 2015, more in section 4.4).

PAPER V argues that the assessment of Icelandic dust on snow/ice surface darkening and melt is currently unavailable and therefore scientific research is critically needed. While transport and deposition of light-absorbing Icelandic volcanic dust can have a significant influence on the cryosphere, in Greenland and elsewhere, it is not included when glacier and ice cap melt rates and deglaciation are investigated. The reasoning is based on the following: Iceland is the most important Arctic dust source, and this dust can be transported over the North Atlantic to Europe and Greenland, the dust-storm frequency is large and many dust-storms take place in winter (dust mixes with snow), the fertilising effect of dust can offer an important nutrient source that enables microorganisms to grow, and other living organisms present in Icelandic dust can also be intercontinentally transported. PAPER V also hypothesises that in the Arctic, Icelandic dust may have a comparable or even larger effect on the cryosphere than soot. The particle-cryosphere interaction is controlled also by the particle properties, which vary according to the origin from the seven major Icelandic dust sources (Arnalds et al. 2016). Hydrophobic particles can concentrate on the surface, whereas hydrophilic particles can be washed down with melt water (Doherty et al. 2013) and play a role in creating environmental conditions within snow/ice that favour the existence of microorganisms. Observations and modeling results on Icelandic dust and cryosphere interactions for the past, present, and future are urgently needed is the message of PAPER V.

4.4 Modeling, remote sensing and Arctic-Antarctic aspects

Modeling and remote sensing aspects are included mostly in PAPER II-III (but also PAPER I and V), and Antarctic aspects in PAPER I. To start with, PAPER I studies whether the empirical data show any relationships that could be used for simple parameterizations. A nonlinear regression between reflectivity and snow depth of melting snow in Sodankylä is found (Eq. 4 and Fig. 9 of PAPER I). Previously Arola et al. (2003) also reported a similar simple nonlinear parametrization and used the relationship of snow depth and albedo for estimating the albedo of snow covered surfaces in their satellite method. PAPER I concludes that empirical data as such can be useful for modeling purposes, as earlier Wiscombe and Warren (1980) had said that only a small number of albedo models had been put forward prior to their model, reflecting the lack of high-

quality data against which to check such a model, and the fact that some of the data are contradictory. The BC snow albedo effects are investigated in PAPER II with the help of measured and SNICAR modeled albedo and ancillary data (Fig. 4.4). The SNICAR model user can give the concentration of BC (ppb, or nanograms of BC per gram of ice) as input. The model uses a MAC scaling factor which is experimental. Using MAC = 1, the model uses the value of 7.5 m^2 g^{-1} at 550 nm for uncoated BC (mimicking hydrophobic particles), and 1.5 for sulfate-coated black carbon (mimicking hydrophilic black carbon). Here SNICAR was used to investigate in which conditions the modeled albedo could match the measured albedo. The measured snow albedo values were unexpectedly low, but considered to be good estimates close to the true albedo, as the values were evidenced by three independent measurement data sets. To mactch the measured albedo to the SNICAR modeled albedo required a MAC multifying factor of 10 (Figure 4.4).

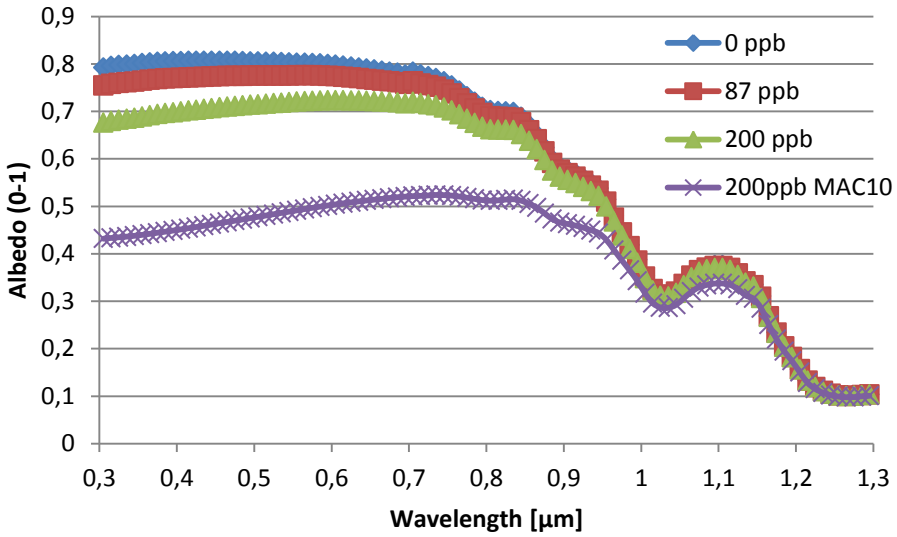

Figure 4.4. The snow albedo spectra at 0.3–1.3 µm simulated for clear sky using the SNICAR model (Flanner et al. 2007). The modeled absorption effects of light-absorbing impurities in snow appear the bigger the shorter the wavelength, and most pronounced at UV. The same spectral absorption feature is also evident for atmospheric absorption of BC (Fig. 9 of Voisin et al. 2012). Realistic parameter values are used as input (SZA = 55 degrees, grain radius 1.5 mm, snow depth 10 cm, snow density 350 kgm^{-3}). The BC and MAC values are then changed to represent the cases of clean snow (blue, 0 ppb), and the EC amount detected using the thermo-optical method (red, 87 ppb). The actual BC concentration in snow, determined by the thermo-optical method, can be assumed (Chow et al. 2001) to be appr. double of the measured EC (green, 200 ppb). To match the measured albedo of ~0.4–0.5 with the modeled, we need a MAC multiplying factor =10 for hydrophobic BC (purple, 200 ppb, MAC 10). Figure 10 of **PAPER II**.

PAPER II states that the diurnal SZA asymmetry in the albedo of melting snow (reported in PAPER I–II) means a potential error in the satellite detected albedo. The RT calculations show that if the 10 % daily melt time asymmetry effect is ignored, an error of

2–4 % in the calculated clear sky downward irradiance is made for one day. This means that if using daily satellite-based albedo data for RT applications, even if the satellite and ground albedo were to match perfectly, there remains an error of the mentioned percentages caused by diurnal snow melting.

Another kind of error source in satellite data is discussed in PAPER V. There the remote sensing results of Polashenski et al. (2015) are cited. They showed that satellite data analysis of Moderate Resolution Imaging Spectrometer (MODIS) surface reflectance from the Terra sensor degradation has important contributions for detecting the Greenland's dry snow zone albedo decline. Polashenski et al. (2015) did not find that enhanced deposition of LAI caused any significant dry snow albedo reduction or melt events, but they acknowledged prior work on GrIS, wherein the impact of MODIS Terra degradation had been concluded as insignificant. Polashenski et al. (2015) agree that part of the dry snow zone albedo decline could be real.

For the SILAM model calculations on the origin of BC in Sodankylä snow in PAPER II, simple rules ("an algorithm") were used to connect the measured BC in snow concentrations to the origins of snow pollution by means of transport modeling. The SILAM footprints were calculated for the "clean" and "dirty" cases (Fig. 9 of PAPER II). The model results show a difference in sensitivity area at Kola Peninsula for clean and dirty footprints. This pattern also agrees with the location of main air pollution sources in the region, mining and refining industries at Kola Peninsula.

Snow density investigated in PAPER III is an important model parameter, because density multiplied by snow depth equals the important climate model parameter of snow water equivalent (SWE).

The Arctic-Antarctic snow albedo aspects are discussed mostly in PAPER I, sections 5.2–5.4. The diurnal decline in albedo and SZA asymmetric albedo of PAPER I, have been found in Antarctic snow by several authors. These SZA asymmetric albedo results are opposite to what is predicted by the theory and have been explained in the Antarctic by changing snow conditions, and diurnal deposition and evaporation of a hoar-frost coating on the snow surface (Pirazzini 2004, Wuttke et al. 2006). Reasons for differences in the Arctic and Antarctic snow albedo are briefly discussed in PAPER I, referring to differences in snow grain sizes, amounts of impurities in snow and air, surface structures, atmospheric moisture, and topography.

5 Summary and conclusions

The Arctic region has warmed more than the global average, a phenomenon known as Arctic amplification. Arrhenius (1896) argued that concentrations of carbon dioxide in the atmosphere could alter the Earth's surface temperature with stronger warming in polar regions due to albedo feedback, i.e., a process where initial warming melts some of the highly reflective snow and ice cover, exposing darker surfaces with stronger absorption of solar energy, leading to further warming and retreat of snow and ice. In reverse, initial cooling leads to increased snow and ice cover, leading to further cooling.

Currently, Arctic amplification is understood to have a variety of causes on different temporal and spatial scales. Albedo feedback is often cited as the main contributor. When dark aerosol particles (BC, OC, dust) are deposited on snow and ice surfaces, the climatic effects are due to reduced albedo and to the induced melt of darker surfaces, which again lowers the albedo and increases melt via the albedo feedback mechanism. In addition to climatic effects, LAI can have, depending on their physical and chemical properties, diverse environmental and hydrological impacts, e.g., in acting as fertilizers or inducing snow and ice melt. The importance of the biological impact on albedo was suggested by Benning et al. (2014), and more recently, on glacier melt by Lutz et al. (2016).

This thesis work has filled in some of the gaps in our knowledge of the effects of LAI on snow in the European Arctic through a series of field and laboratory experiments and analysis of the resulting data, including modeling. The thesis suggests that Icelandic dust in the cryosphere can be one possible cause of Arctic amplification. Icelandic dust is one of the most abundant dust sources in the climate system, and there are about 135 dust events per annum. It has been increasingly recognized that dust produced at high latitude and in cold environments may extend beyond the local source area and have regional or global significance in the Earth system. This thesis states that Iceland is the most important Arctic dust source, but a scientific assessment of its impacts on the cryosphere is currently unavailable, and more scientific results are urgently needed to investigate the role of Icelandic dust in Iceland and elsewhere in the past, present, and future.

As the assessment of the cryospheric role of Icelandic dust is currently missing (referring to PAPER V and Bullard et al. 2016), it also means that until now, Icelandic dust has often been ignored in models and dust effect studies. In the Arctic, Icelandic dust particles can influence both the temperature due to their radiative effects and the albedo feedback effect when deposited.

In terms of radiation budget and climate effects, information on the total shortwave albedo, integrated over the whole solar spectrum and the upper hemisphere, is required. The data acquired within the thesis work on UV and VIS albedo and LAI in snow can be used to calculate the spectral albedo and radiative forcing (i.e., climate impact) of LAI (BC, OC, dust) in snow. The radiative forcing can be inferred from modeling constrained by the in situ data of LAI using the SNICAR and LibRadtran RT models, following the

approach presented in Kaspari et al. (2015), for example. There, the reflected fluxes were calculated for clean and LAI-laden runs integrated over the day to produce all-sky 12 h daily mean radiative forcings.

The atmosphere-cryosphere interactions include a number of processes that are not completely understood. This thesis suggests a "BC density effect" in addition to the "BC albedo effect." To further improve our understanding of the role of LAI in the Arctic feedback processes (positive and negative), we need both long-term observations and modeling. This would require experimental, in situ, and satellite observations of LAI sources, transport, and deposition, and studies on the particle properties and their cryospheric impacts, combined with radiative forcing, long-range transport and climate modeling. In addition, Arctic amplification has inter-connected consequences for the biosphere (e.g., so-called Arctic greening), carbon and hydrogen cycles, and human society. The feedback loops therefore essentially include atmospheric-cryospheric-biosphere-human activities and society interactions.

The results of this thesis contribute to the knowledge on interlinks and feedbacks in light-absorbing impurities and cryosphere interactions. The main findings of this thesis are:

1. Light-absorbing impurities and snow albedo and melt *(the scientific question Q1 of this Thesis):*

- the in situ snow UV and VIS albedo in Sodankylä, north of the Arctic Circle, were in the melting season lower (0.5–0.8) than expected (> 0.9) on the basis of literature (Grenfell et al. 1994).
- the low albedo values, confirmed by three independent measurement set ups, were explained by large snow grain sizes (up to 3 mm in diameter), melt water surrounding the snow grains, and absorption caused by impurities (87 ppb BC and 2894 ppb OC at the time of the albedo measurements)
- diurnal SZA asymmetry in the Arctic snow albedo, during snow melt, was detected opposite to the theory of the SZA dependent U-shape of the albedo signal (Briegleb et al. 1986)
- the SZA asymmetry was explained to be due to changes in the properties of intensively melting snow, where the diurnal albedo decline dominates over the SZA dependency
- spectral change in the measured data was the greater the shorter the wavelength. This is consistent with the theoretical results of Warren and Wiscombe (1980), which show that absorption due to snow impurities increases with decreasing wavelength
- observations on impurities on the surface snow when snow melts (e.g., in case of Icelandic volcanic sand, suggesting hydrophobic particle properties)
- observations on clumping of particles when on melting snow or ice surface
- observations on impurities induced cryoconite holes on melting snow and ice.

2. BC and OC in snow and their origin *(the scientific question Q2 of this Thesis)*

- BC contents of the surface snow layer, sampled weekly during snow time in 2009 - 2011 at Sodankylä, were found higher (up to 106 ppb) than expected (up to 60 ppb during melt, Doherty et al. 2013)

- higher BC concentrations in snow in spring time suggested surface accumulation of hydrophobic BC during snow melt
- some of the high BC concentrations were found to be due to anthropogenic soot transported from the Kola Peninsula, Russia, with industrial activities. This origin was suggested by SILAM footprint calculations utilizing the measured BC in snow data and meteorological data on rainfall, combined with *a priori* threshold values based on literature (Doherty et al. 2010 and 2013), and a rule relating the snow sample collection time with the occurrence of rain events
- the origin of OC (max values > 2000 ppb) can be anthropogenic or natural, and may include pollen, seeds, lichens, natural litter or microorganisms that reside in snow and ice.

3. LAI and snow density *(the scientific question Q3 of this Thesis):*

- a new hypothesis on the snow density effects of light-absorbing impurities, an important quantity for climate modeling and remote sensing, was presented
- three potential processes were suggested to explain the ”BC density effect”:
    - a semi-direct effect of absorbing impurities, where absorbing impurities would cause melt and/or evaporation from the liquid phase and sublimation from the solid phase of the surrounding snow, resulting in air pockets around the impurities, and thus lower snow density;
    - effect on the adhesion between liquid water and snow grains, where BC reduces adhesion, and the liquid-water holding capacity decreases; or
    - effect on the snow grain size, where absorbing impurities increase the melting and metamorphosis processes, resulting in larger snow grains, which lower the water retention capacity;
- experimental results show that dirty snow release melt water quicker than cleaner snow.

4. Cryospheric effects of Icelandic volcanic dust *(the scientific question Q4 of this Thesis):*

- a scientific assessment of Icelandic dust impacts on the cryosphere is currently unavailable, although Iceland is the most important Arctic dust source, and scientific results are urgently needed to investigate the role of Icelandic dust in Iceland and elsewhere, in the past, present and future
- the experimental results on Icelandic volcanic ash showed that Eyjafjällajökull ash with grain size smaller than 500 μm insulated the ice below at a thickness of 9–15 mm (called as ‘critical thickness'). For the 90 μm grain size, the insulation thickness was 13 mm. The maximum melt occurred at thickness of 1mm for the larger particles, and at the thickness of < 1–2 mm for the smaller particles (called as ‘effective thickness'). Earlier, similar threshold dust layer thickness values have been given for Mt St Helens (1980) ash, and Hekla (1947) tephra, for example (references given in PAPER IV)
- these results were the first ones reported for the Eyjafjällajökull ash
- in Iceland, the dust layers in the nature can be from mm scale up to tens of meters. These results suggest increased melt in areas with smaller amounts of dust, further away from the eruption, inside Iceland and elsewhere. In literature, long-range transported Icelandic dust has been reported to be found even over the Atlantic (Prospero et al. 2012).

5. Challenges, needs and possibilities in modeling and remote sensing approaches and in bipolar Arctic-Antarctic research (*the scientific question Q5 of this Thesis):*

- the need to understand ground truth processes was shown, as the measured in situ SZA asymmetric albedo was found to result in a 2–4 % daily error for the daily satellite snow albedo estimates
- the snow albedo model results indicated that the biggest snow albedo changes due to BC are expected in the UV part of the EM spectrum, and that the MAC assumptions significantly influence on the simulated spectral albedo values for dirty snow
- clumping mechanism of impurities on snow surface was observed (while, e.g., Schwarz et al. (2013) assume that no BC agglomeration in snow takes place)
- a method to connect the observed BC contents of snow with the origin of pollution for the dirty snow samples using SILAM footprint calculations indicated the areas that were likely to be responsible for the origin of the pollution
- Arctic work can be used for the benefit of the Antartic research. The methods can first be developed and tested in the Arctic, before including them in the Antarctic work, and thereafter the same methods used in bipolar research can give in-depth understanding. The diurnal decline in the albedo and the SZA asymmetric albedo detected in PAPER I, have been found in Antarctic snow and explained in the Antarctic by changing snow conditions, and diurnal deposition and evaporation of a hoar-frost coating on the snow surface (Pirazzini 2004, Wuttke et al. 2006). Reasons for differences in the Arctic and Antarctic snow albedo were discussed in PAPER I, referring to differences in snow grain sizes, amounts of impurities in snow and air, surface structures, atmospheric moisture, and topography.

Warren and Wiscombe (1980) urged high-quality albedo data against which to check the modeled albedo. The need for high-quality in situ data for model and satellite data verification exists. Both the model and the remote sensing approaches require empirical measurement data. Various types of models related to the cryosphere–atmosphere interactions, from the surface albedo to Climate and Earth System Modeling, are under continuous development. Also measurement devices, both ground-based and satellite, continue to improve by their spatial and spectral resolutions and accuracy. A lot of effort is also put on developing algorithms to retrieve various properties of environmentally important parameters, e.g., in satellite aerosol remote sensing (Kokhanovsky and Leeuw 2009). Both the in situ radiometer measurements as well as the radiometers onboard satellites suffer from various errors and uncertainties. PAPER I discussed errors and uncertainties related to the Sodankylä SL501 albedo data, and how these challenges were taken care of. Yet, even data correction for known errors is not always enough. PAPER II showed that a 10 % diurnal SZA asymmetry in the melting snow albedo can cause a 2–4 % error in the satellite albedo estimates, even when satellite data are corrected for their known errors. The observed SZA asymmetry case demonstrates the need for further work on identifying, quantifying and parameterizing ground truth processes, especially when contradicting theory, and these to be implemented in models.

6 Future aspects

6.1 Broader research field and multi-method approaches

The scientific focus of this thesis was on effects of black carbon, organic carbon and Icelandic volcanic dust on Arctic snow and ice optical properties, melt and density, as discussed in connection with sources of emissions, long-range transport and deposition. These atmospheric aerosol particles originate from anthropogenic or natural sources. Further work towards better understanding of the Arctic environment includes various research questions within the atmospheric–cryospheric interactions. The most recent internationally recognized hot topics include at least the role of various light-absorbing impurities in the Arctic amplification, high-latitude dust in the Earth system, biological impacts in the cryosphere, as well as darkening of Greenland.

6.1.1 Experiments and modeling

Future work aiming at improving any aspect related to the SNICAR snow albedo model (Flanner et al. 2007) could benefit also other models where SNICAR is part of, including Climate and Earth System Models.

Such an improvement possibility could exist in the representation of the optical properties of Icelandic dust particles, which depend strongly on source material. This knowledge could be useful for other models, too. Volcanic ash exhibits large optical variability, depending on volcanic mineralogy and type of eruption. According to the SNICAR model documentation, the optical properties of dust are designed to represent "global-mean" characteristics as closely as possible, where a mixture of quartz, limestone, montmorillonite, illite, and hematite is assumed. E.g., in case of dust particles with a large proportion of strongly-absorbing hematite, a larger impact on the snow albedo is expected as compared to the dust in SNICAR. The properties of volcanic ash particles in SNICAR are derived from measurements of ash particles from the Mount St. Helens, Washington, in the Pacific Northwest region of the United States. Therefore, optical characterization of the Icelandic dust particles, i.e., providing data on wavelength dependent refractive indeces, from the seven major dust sources could serve as an improvement for SNICAR.

It could also be worth investigating if the detected changes in the albedo due to LAI (BC, OC, dust) could be further used in regional climate models to compare model runs with and without LAI, to gain an estimate on the LAI albedo impact in the Arctic region. According to Dr. Petri Räsisänen (FMI), The ability for dust emissions to change with changing climate means that they should be made dependent on weather/climate

conditions (e.g., wind and presence of snow on ground) (pers.comm. Dr. Petri Räsisänen, FMI, September 2016).

Organic carbon absorption in the SNICAR modeled snow albedo offers an unsolved question, too. Based on the results presented in PAPER II, I currently assume some moderate or strongly absorbing organic carbon to be present in the snow at the time of the albedo measurements. The organic carbon in the snow can be an important source of absorption. The OC absorption could also partly explain the high MAC value needed for BC to match the measured low albedo values with the SNICAR simulated albedo values. According to Dr. Flanner, the OC that is included in SNICAR is only weakly absorbing, and it is probably too weak to represent the OC that was present in the snow when the low albedo values were measured. Furthermore, it may be difficult to represent OC/brown carbon in the SNICAR model, because the particles exhibit large variability in optical properties, and thus we cannot adequately capture this variability with only one type of OC (Dr. Flanner, pers.comm. 27 May 2016). To derive optical properties for a special version of OC (that is considered representative of the OC in the snow), spectrally-resolved estimates of the "target" MAC would be required. The already existing data could be utilized together with new measurements for the benefit of the SNICAR model development and OC representation in the SNICAR.

The biological impact on the snow and ice albedo and melt has been indicated in Benning et al. (2014) and Lutz et al. (2016). Our Arctic observations and measurements in Sodankylä, Finland, and in Iceland on OC contents in snow also suggest a possibly significant role of organic biological compounds affecting the snow/ice albedo. Our new Icelandic–Finnish co-operative analysis results on BC/OC in snow and glacier ice in Iceland will be the first results for snow and ice in Iceland, as far as we know. The preliminary results suggest very small amounts of BC in snow, and larger OC contents. Also, new understanding on the Sodankylä OC results, i.e., the organic carbon contents in our snow samples, was gained when our recent first microscope investigations on surface snow samples from Sodankylä snow revealed algae and other organic material on the snow surface (Fig. 6.1, photo on the left). In addition, the weekly filter samples were found to contain organic trash (Fig. 6.1, second photo from the left).

Greenland's darkening is currently an unsolved question. Forest fires have also been shown to be an infrequent, but sometimes very large, source of BC deposition to Greenland (e.g. McConnell et al. 2007). To investigate the reasons behind Greenland's darkening, and the albedo feedback (Box et al. 2012), sampling of snow for BC and Icelandic dust particle contents could be undertaken. These results could then be combined with the study of the origin of the impurities in a similar way as presented in PAPER II, using SILAM footprint calculations. Earlier, Greenland Ice Sheet snow was found to have the lowest BC content of the Northern Hemisphere (3 ppb, Doherty et al. 2010). In the percolation zone and the wet-snow zone of the Greenland Ice Sheet, the BC was accumulated in the surface snow due to snow melt, with concentrations of 10–20 ppb (Doherty et al. 2010). According to Warren (2013), the problems of snow thinness and patchiness are nonexistent on the Greenland Ice Sheet, where the snow surface is horizontal, uniform, deep, and unvegetated. The most favorable location for remote sensing would be the wet snow zone of Greenland late in the melting season, when BC has become concentrated at the surface.

The hydrophilic and hydrophobic properties of LAPs, and BC particle size in snow can play a big role in the cryosphere–atmosphere interactions and should be studied more. The SP2 and NIOSH methods are currently in use at FMI, and a comparison data set has been collected for a method comparison. Interesting aspects are also related to the fact that BC is different by its size in the air and snow (Schwarz et al. 2013).

6.2 Experiments, modeling and satellite approaches

The need for understanding the basic processes when utilizing satellite data is presented in our recent joint-paper of Peltoniemi et al. (2015) on BRDF changes for contaminated snow. The work shows that the surface of dirty snow remains the darkest when the reflectance is measured at nadir, but at larger zenith angles the surface of the contaminated snow appears almost as white as clean snow. This means that for an observer at the surface, the darkening caused by impurities can be completely invisible, overestimating the albedo, but a nadir-observing satellite sees the darkest points, underestimating the albedo. These observations give reasoning for future investigations on satellite data to compare nadir pixels with non-nadir data, combined with BRDF properties of various impurities on snow and ice surfaces.

The UV part of the EM spectrum can be utilized for detecting LAPs in snow. Painter et al. (2007) observed the most pronounced decrease towards the UV portion of the spectrum due to dust deposition. The spectral absorption properties of soot and Icelandic dust particles alone and on snow are presented in Peltoniemi et al. (2015), too. Current satellite UV algorithms demand better information on the UV albedo, especially for the land when covered by snow (e.g., Arola et al. 2003, Tanskanen and Manninen 2007). The snow albedo changes due to impurities are usually detected at the visible and near-infrared wavelengths, excluding the ultraviolet (UV, $\lambda < 400$ nm). However, as LAPs are often strong UV absorbers, albedo changes could therefore be first detectable in the UV.

Combining UV and BRDF effects for satellite detection of impurities in the cryosphere could serve as an interesting option to be investigated. With a combination of optimal spectral and directional information, it could be tested if a) smaller concentrations than 1000 ppb of BC in snow, referring to Warren (2013), or b) Icelandic volcanic dust in snow, can be detected by remote sensing.

The Sodankylä Arctic snow SL501 albedo data have been compared in international co-operation with the Antarctic albedo data of the Neumeyer station (Meinander et al. 2009), where SZA asymmetry were found in both data sets. The Arctic data can be compared with our Antarctic SL501 albedo data available from Marambio since 2013 (FINNARP 2014). These bipolar irradiance data can also be used for satellite data validation. The first comparison I made for the Marambio NILU-UV data with the OMI satellite overpass data showed a difficulty in seprating clouds from snow in the satellite algorithm (FINNARP 2014). Moreover, Marambio offers a climatically interesting location to investigate the albedo of melting snow and duration of snow free periods, as the Antarctic Peninsula has experienced warming at rates several times the global mean (Trenberth et al. 2007).

For wind-blown Icelandic dust, satellite data can be employed together with AWS data to detect where and when dust events take place, and long-range transport calculations to show where the dust is transported and deposited. For Greenland's darkening, we would also need empirical studies on Icelandic dust and snow/ice interactions to understand the effects of Icelandic dust deposits in Greenland.

6.2 Practical considerations on snow experiments and monitoring

There are many advantages in snow research in Finland. First of all, there are large remote almost untouched areas with clean snow and clean air, and snow melts every year, which enables climate change related experiments and long-term monitoring on naturally melting snow. The topography of Finland is relatively flat, which can make the understanding of processes easier. Finland has five out of the six global snow classes (Sturm et al. 1995), only alpine snow missing. Sodankylä, from where most of the thesis data originated, belongs to the Taiga snow class. For naturally melting snow, effects of snow drift on the albedo results can be assumed smaller compared to places elsewhere with snowdrift affecting results due to non-melting snow and hard winds. Suggestions for practical work related to snow experiments and snow monitoring in Finland and elsewhere include:

1. To identify locally the origin of BC in snow, our findings in PAPER II suggest benefits when using snow sampling and EC/OC analysis combined with the SILAM footprint calculations. This approach can provide relevant information on the origin of the BC in snow complementary to atmospheric BC measurements or other modeling approaches (e.g., Hienola et al. 2013). The SILAM footprint approach (Fig. 3.5 of this thesis) is planned to be applied to investigate BC in Icelandic snow, where the first snow samples have been collected in March 2016.

2. The SL501 snow UV albedo data included in PAPER I–II now offers a 10 year time series, available for validating the SNICAR model. Since 2009, these albedo data are combined with EC/OC in snow. The five years EC/OC data (2009-2013) suggest a spring time snow melt accumulation of the surface layer BC contents similarly to the shorter data set of PAPER II. Combining these EC/OC data with the UV albedo data and SILAM footprint calculations is in preparation, too.

3. To test the hypothesis on the BC density effect presented in PAPER III and to investigate under which circustances this hypothesis is valid, we have collected more materials from Iceland and elsewhere in Finnish–Icelandic–Chinese co-operation, within the "Pan-Eurasian Experiment" (PEEX) of the University of Helsinki.

4. Separating soot and dust effects could be further investigated using the materials of the experiments of PAPER III-IV. The comparisons of effects of soot and dust on snow melt, albedo and density can be investigated based on these materials

5. As a small practical detail of the consequence of the work presented in PAPER II, I suggested to use a sieve away (with known grid size) the biggest trash while filtering Sodankylä snow for impurity analysis. This is the current Sodankylä practice, and this simple improvment could benefit any similar work elsewhere, too.

6. Here use was made from long-term measurements as well as experiments during shorter periods. The radiometers used for lomg-term albedo measurements are applicable in the field, but instrumentation developed especially for field use is available, too. An ASD spectrometer (www.asdi.com) is one instrument often applied in the field (currently in my use at FMI). Its main advantage is the light weight and the quick measurement compared to, e.g., operational albedo sensors, or Bentham with two input optics. A remote cosine response device can be used for measuring BHR. Alternatively, smaller field-of-view reflectance can be computed with measurements from both the unknown material and a reference material, i.e., Spectralon reference panel with approximately 100 % reflectance across the entire spectrum. A contact probe can be attached to an ASD spectrometer to study particle reflectance properties with and without snow (Figure 6.1).

6.3 What is the role of Icelandic dust in the Arctic cryosphere?

Currently, only few studies on effects of Icelandic volcanic dust on the snow and ice albedo and melt have been published (Dagsson-Waldhauserova et al. 2015, Dragosics et al. 2016, Meinander et al. 2016, Svensson et al. 2015, Peltoniemi et al. 2015), although the need for its scientific evidence is high (Myhre et al. 2013). Ecological and climatological significances of volcanic dust events can be variable depending on the properties of the particles; such as their physical properties, chemical composition, and capability to be transported. About half of the annual dust events in the southern part of Iceland take place at sub-zero temperatures, when dust may be mixed with snow (Dagsson-Waldhauserova et al. 2015). Our joint paper (Dagsson-Waldhauserova et al. 2015) shows that the amounts of dust that are transported with wind can't be ignored in Iceland. Icelandic dust is a natural source of LAI, where the dust storm frequency and severerity can be connected to climate change. If more extreme winds would follow as a result of climate change, then more severe Icelandic dust events would take place more often, too.

The glaciers are melting rapidly in Iceland. I recently had the chance to visit a glacier for the first time (Fig. 6.1). The melt of that Solheimajökull-glacier is unbelievable: in 20 years it has shrunk from its southwestern outlet by appr. 900 m (pers.comm. Dr. Dagsson-Waldhauserova 9.6.2016, http://www.ruv.is/frett/hopadi-um-887-metra-en-ekki-240). The assessment of effects of the Icelandic volcanic dust is missing and more research work is urgently needed. Related to Icelandic dust and cryoconite, PAPER V brings out the fact that living organisms present in Icelandic dust (Kelly et al. 2014) can also be intercontinentally transported (Gorbushina et al. 2007, de Leeuw et al. 2014). Hence, the biological impact should be included in the investigations.

For studies of effects of light-absorbing impurities on the Arctic cryosphere, Iceland offers an important hot spot in Europe. The reflectance and albedo properties of snow and various particles (alone and together) can be further connected with their BRDF properties (Aoki et al. 2000, Peltoniemi et al. 2015), as well as SEM analysis on the shape, size and mineral contents of BC, OC, or mineral and volcanic dust particles, not only for Iceland but also elsewhere (e.g., Tirsch et al. 2012), up to Hawaiian volcanic particles or dust particles of the Mars planet.

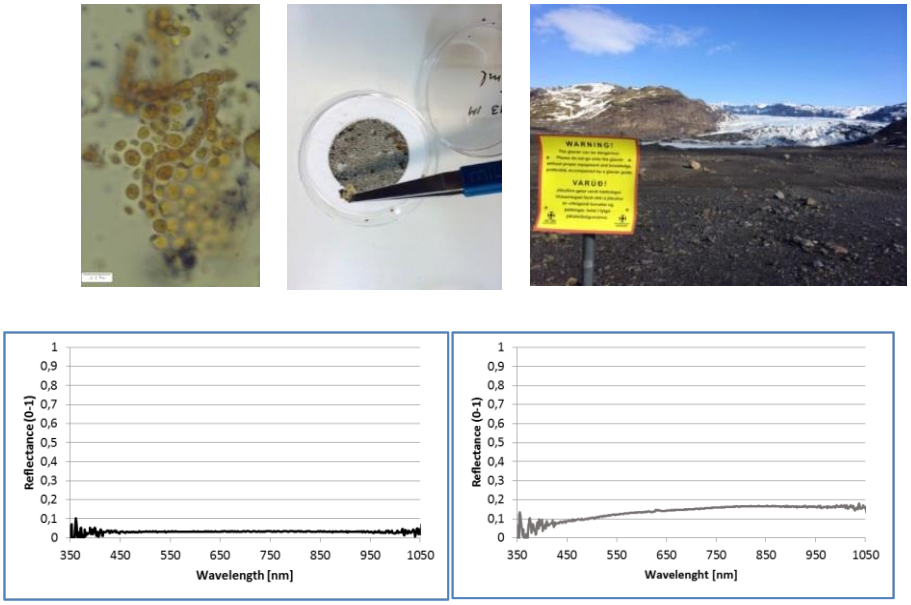

Figure 6.1. The role of organic carbon and Icelandic dust in the Arctic amplification are questions that have received only little scientific attention until now. The OC content in Sodankylä snow samples has been found to be partly due to algae (up left, fist Sodankylä snow microscopic results, photo by Anke Kremp, SYKE, published with the permission of A. Kremp) pollens and other organisms in the snow, as well as trash like needles on the filter (up middle, photo O. Meinander). The mass balance of the glacier Solheimajökull in Iceland is negative and it has been shrinking during the last 20 years by 900 meters from its southwestern corner (up right, photo O.Meinander, March 2016). Spectral reflectance of Icelandic volcanic sand particles (a dark mixture of the volcanic ash of glaciofluvial nature, originating from under the Myrdalsjökull glacier, which was likely mixed with the ash of the Eyjafjallajökull eruption in 2010, and the Grimsvötn eruption in 2011), and Icelandic glaciogenic silt particles collected by the river Mulakvisl, originating from the Myrdalsjökull glacier, possible to be deposited on the local glaciers, as well as long-range transported, measured with a contact probe attached to an ASD spectrometer (O.Meinander).

Acknowledgements

I gratefully acknowledge the Academy of Finland (project "Arctic Absorbing Aerosols and Albedo of Snow" (A^4), decision 254195, and project "Novel Assessment of Black Carbon in the Eurasian Arctic: From Historical Concentrations and Sources to Future Climate Impacts" (NABCEA), decision 296302); the CRAICC Fellowship 2015/2016 of the Nordic Top-level Research Initiative (TRI) project Nordic Centre of Excellence NCoE CRAICC (Cryosphere-atmosphere interactions in a changing Arctic climate); the Finnish Centre on Excellence FCoE ATM in Atmospheric Science funded by the Finnish Academy of Sciences Excellence (project no. 272041); the personal award from the US Alexander Goetz Instrument Support Program (AGISP) for "Arctic Snow Reflectance and Albedo Affected by Black Carbon"; the European Science Foundation ESF Science prize for my poster on Albedo of Arctic Snow; the University of Helsinki Doctoral Program in Atmospheric Sciences (ATM-DP); the EU COST-STSM-FP0903-10960 for "Reflectance and albedo of snow and vegetation for environmental studies"; and the EU COST-STSM-ES1404 for "Ice and Snow Observations in Iceland: Detecting effects of volcanic dust on snow and ice".

References

Aamaas, B., Bøggild, C. E., Stordal, F., Berntsen, T., Holḿen K. & Strom, J. Elemental carbon deposition to Svalbard snow from Norwegian settlements and long-range transport, Tellus, 63B, 340–351, doi:10.1111/j.1600-0889.2011.00531, 2011.

Adler, G., Riziq, A.A., Erlick, C. & Rudich, Y. Effect of intrinsic organic carbon on the optical properties of fresh diesel soot, PNAS 2010 107,15, 6699-6704, doi:10.1073/pnas.0903311106, 2009.

Agrawal, B.N. Design of geostationary spacegraft, Prentice-Hall, USA, 450 p, 1986.

AMAP. Black carbon and ozone as Arctic climate forcers, Arctic Monitoring and Assessment Programme (AMAP), Oslo, Norway. vii + 116 pp. ISBN – 978-82-7971-092-9, 2015.

Andrady, A. L., Torikai, A., Redhwi, H. H., Pandey, K. K. & Gies, P. Consequences of stratospheric ozone depletion and climate change on the use of materials, Photochemical & Photobiological Sciences, 14, 1, 170-184, 2015.

Aoki, T., Fukabori, M., Hachikubo, A., Tachibana, Y. & Nishio, F. Effects of snow physical parameters on spectral albedo and bidirectional reflectance of snow, J. Geophys. Res.,105, 10219–10236, 2000.

Arnalds, O. Dust sources and deposition of aeolian materials in Iceland, Icel. Agr. Sci., 23, 3–21, 2010.

Arnalds O., Dagsson-Waldhauserova P. & Olafsson H. The Icelandic volcanic aeolian environment: Processes and impacts - A review. Aeolian Research, doi:10.1016/.j.aeolia.2016.01.004, 2016.

Arola, A., Kaurola, J., Koskinen, L., Tanskanen, A., Tikkanen, T., Taalas, P., Herman, J.R., Krotkov, N. & Fioletov V. A new approach to estimating the albedo for snow-covered surfaces in the satellite UV method, J. Geophys. Res., 108, D17, 4531, doi:10.1029/2003JD003492, 2003.

Arrhenius, S. On the influence of carbonic acid in the air upon the temperature of the ground, Philos.Mag.J.Sci. 5, 237-276, 1896.

Benning, L. G., Anesio, A.M., Lutz, S. & Tranter, M. Biological impact on Greenland's albedo, Nature Geoscience 7, 691, 2014.

Birch, M. E. Diesel Particulate Matter (as Elemental carbon) Method 5040, in NIOSH Manual of Analytical Methods, National Institute of Occupational Safety and Health, Cincinnati, Ohio, 2003.

Birch, M. E. & Cary, R. A. Elemental carbon-based method for monitoring occupational exposures to particulate diesel exhaust, Aerosol Sci. Technol., 25, 221–241, 1996.

Bird, R.E. & Riordan, C. Simple solar spectral model for direct and diffuse irradiance on horizontal and tilted planes at the Earth's surface for cloudless atmospheres. J. Clim. Appl. Meteorol. 25, 87-97, 1986.

Blumthaler, M. & Ambach, W. Solar UV Albedo of various surfaces, Photochemistry and Photobiology, 48, 1, 85–88, 1988.

Bond, T. C. & Bergstrom, R.W. Light absorption by carbonaceous particles: An investigative review, Aerosol Sci. Technol., 40, 1, 27-67, doi: 10.1080/02786820500421521, 2006.

Bond, T. C., Habib G. & Bergstrom, R.W. Limitations in the enhancement of visible light absorption due to mixing state, J. Geophys. Res., 111, D20211, doi: 10.1029/2006JD00731, 2006.

Bond, T.C., Doherty, S.J., Fahey, D.W., Forster, P.M., Berntsen, T., DeAngelo, B.J., Flanner, M.G., Ghan, S., Kärcher, B., Koch, D., Kinne, S., Kondo, Y., Quinn, P.K., Sarofim, M.C., Schultz, M.G., Schulz, M., Venkataraman, C., Zhang, H., Zhang, S., Bellouin, N., Guttikunda, S.K., Hopke, Jacobson, P.K., Kaiser, J.W., Klimont, Z., Lohmann, U., Schwarz, J.P., Shindell, D., Storelvmo, T., Warren, S.G. & Zender, C.S. Bounding the role of black carbon in the climate system: A scientific assessment, J. Geophys. Res. Atmos., 118, 11, 5380-5552, doi:10.1002/jgrd.50171, 2013.

Box, J. E., Fettweis, X., Stroeve, J. C., Tedesco, M., Hall, D. K. & Steffen, K. Greenland ice sheet albedo feedback: thermodynamics and atmospheric drivers, The Cryosphere, 6, 821-839, doi:10.5194/tc-6-821-2012, 2012.

Briegleb, B.P., Minnis, P., Ramanathan, V. & Harrison, E. Comparison of Regional Clear Sky Albedos Inferred from satellite Obervations and Model Computations, Journal of Climate and Applied Meteorology, 25, 214-, 1986.

Brock, B., Rivera, A., Casassa, G., Bown, F. & Acuñn, C. The surface energy balance of an active ice-covered volcano: Villarrica volcano, southern Chile, Ann. Glaciol., 45,1, 104–114, 2007.

Bullard, J. E., Baddock, M.,Bradwell, T.,Crusius, J.,Darlington, E. Gaiero, D., Gassó, S.,Gisladottir, G.,Hodgkins, R.,McCulloch, R. McKenna-Neuman, C. Mockford, T., Stewart, H. & Thorsteinsson, T., High-latitude dust in the Earth system, Rev. Geophys., 54, 447–485, doi:10.1002/2016RG000518, 2016.

Chow, J.C., Watson, J.G., Crow, D., Lowenthal, D.H. & Merrifield, T. Comparison of IMPROVE and NIOSH carbon measurements. Aerosol Sci. Technol., 34, 1, 23-34, 2001.

Clarke, A. D. & Noone, K. J. Soot in the Arctic snowpack—a cause for perturbations in radiative-transfer, Atmos. Environ. 19, 2045–2053, 1985.

Dadic, R., Mullen, P. C., Schneebeli, M., Brandt, R. E., and Warren, S. G.: Effects of bubbles, cracks, and volcanic tephra on the spectral albedo of bare ice near the TransantArctic Mountains: Implications for sea glaciers on Snowball Earth, J. Geophys. Res. Earth, 118, 1658–1676, doi: 10.1002/jgrf.20098, 2013.

Dagsson-Waldhauserova, P., Arnalds, O. & Olafsson, H. Long-term variability of dust events in Iceland, Atmos. Chem. Phys., 14, 13411-13422, doi:10.5194/acp-14-13411-2014, 2014.

Dagsson-Waldhauserova, P., Arnalds, O., Olafsson, H., Skrabalova, L., Sigurdardottir, G.M., Branis, M., Hladil, J., Skala, R., Navratil, T., Chadimova, L., von Lowis of Menar, S., Thorsteinsson, T., Carlsen, H.K. & Jonsdottir, I. Physical properties of suspended dust during moist and low-wind conditions in Iceland, Icelandic Agricultural Sciences 27, 25-39, 2014.

Dagsson-Waldhauserova, P., Arnalds, O., Olafsson, H., Hladil, J., Skala, R., Navratil, T., Chadimova, L. & Meinander, O. Snow-Dust Storm: Unique case study from Iceland, March 6-7, 2013, Aeolian Research, doi: 10.1016/j.aeolia.2014.11.001, 2015.

de Leeuw G., Guieu, C., Arneth, A., Bellouin, N., Bopp, L., Boyd, P.W., Denier van der Gon, H.A.C., Desboeufs, K.V., Dulac, F., Facchini, M.C., Gantt, B., Langmann, B., Mahowald, N.M., Maranón, E., O'Dowd, C., Olgun, N., Pulido-Villena, E., Rinaldi, M., Stephanou, E.G. & Wagener, T. Chapter Ocean-Atmosphere Interactions of Gases and Particles, In Liss, P.S. & Johnson, M.T. (eds), Ocean–Atmosphere Interactions of Particles, Part of the series Springer Earth System Sciences, pp. 171-246, ISBN 978-3-642-25642-4, doi:10.1007/978-3-642-25643-1, 2014.

Di Mauro, B., Fava, F., Ferrero, L., Garzonio, R., Baccolo, G., Delmonte, B. & Colombo, R. Mineral dust impact on snow radiative properties in the European Alps combining ground, UAV, and satellite observations, J. Geophys. Res. Atmos., 120, 6080–6097. doi: 10.1002/2015JD023287, 2015.

Doherty, S. J., Warren, S. G., Grenfell, T. C., Clarke, A. D. & Brandt, R. E. Light-absorbing impurities in Arctic snow, Atmos. Chem. Phys., 10, 11647-11680, doi:10.5194/acp-10-11647-2010, 2010.

Doherty, S. J., Grenfell, T.C., Forsström, S., Hegg, D.L., Brandt, R.E. & Warren, S.G. Observed vertical redistribution of black carbon and other insoluble light-absorbing particles in melting snow, J. Geophys. Res.Atmos.,118, doi:10.1002/jgrd.50235, 2013.

Doherty, S. J., Hegg, D.A., Johnson, J.E. , Quinn, P.K., Schwarz, J.P., Dang, C. & Warren, S.G. Causes of variability in light absorption by particles in snow at sites in Idaho and Utah, J. Geophys. Res. Atmos., 121, doi:10.1002/2015JD024375, 2016.

Dumont, M., Brun, E., Picard, G., Michou, M., Libois, Q., Petit, J.-R., Geyer, M., Morin, S. & Josse, B. Contribution of light-absorbing impurities in snow to Greenland's darkening since2009, Nat. Geosci., 7, 509–512, doi:10.1038/ngeo2180, 2014.

Fierz, C., Armstrong, R. L., Durand, Y., Etchevers, P., Greene, E., McClung, D. M., Nishimura, K., Satyawali, P. K. & Sokratov, S. A. The International Classification for Seasonal Snow on the Ground. IHP-VII Technical Documents in Hydrology, no. 83, IACS Contribution no. 1, UNESCO-IHP, Paris,http://unesdoc.unesco.org/images/0018/001864/186462e.pdf, 2009.

FINNARP. Science and support in Antarctica, ISBN 978-951-697-841-6, 2014.

Flanner, M. G., Zender, C. S., Randerson, J. T. & Rasch, P. T. Present day climate forcing and response from black carbon in snow, J. Geophys. Res., 112, D11202, doi:10.1029/2006JD008003, 2007.

Flanner, M. G. Arctic climate sensitivity to local black carbon, J. Geophys. Res., 118, 1840-1851, doi:10.1002/jgrd.50176, 2013.

Forsström, S., Ström J., Pedersen, C.A., Isaksson, E. & Gerland, S. Elemental carbon distribution in Svalbard snow, J. Geophys. Res., 114, D19112, doi:10.1029/2008JD011480, 2009.

Forsström, S., Isaksson, E., Skeie, R.B., Ström, J., Pedersen, C.A., Hudson, S.R., Berntsen, T.K., Lihavainen, H., Godtliebsen, F. & Gerland, S. Elemental carbon measurements in European Arctic snow packs, J. Geophys. Res. Atmos., 118, 13,614–13, 627, doi:10.1002/2013JD019886.2013, 2013.

France, J. L., Reay, H. J., King, M. D., Voisin, D., Jacobi, H., Beine, H. J., Anastasio, C., MacArthur, A. & Lee-Taylor, J. Hydroxylradical and NOx production rates, black carbon concentrations and light-absorbing impurities in snow from field measurements of light penetration and nadir reflectivity of on-shore and offshore coastal Alaskan snow, J. Geophys. Res., 117, D00R12, doi:10.1029/2011JD016639, 2012.

Gabbi, J., Huss, M., Bauder, A., Cao, F. & Schwikowski, M. The impact of Saharan dust and black carbon on albedo and long-term mass balance of an Alpine glacier, The Cryosphere, 9, 1385-1400, doi:10.5194/tc-9-1385-2015, 2015.

Gallet, J.-C., Domine, F. & Dumont, M. Measuring the specific surface area of wet snow using 1310 nm reflectance, The Cryosphere, 8, 1139-1148, doi:10.5194/tc-8-1139-2014, 2014.

Gardner, A. S. & Sharp, M.J. A review of snow and ice albedo and the development of a new physically based broadband albedo parameterization, J. Geophys. Res. 115, F01009, doi:10.1029/2009JF001444, 2010.

Garratt J.R. The atmospheric boundary layer, Cambridge University Press, 1992. Pp. 316, ISBN 0 521 38052 9, 1992.

Gautam, R., Hsu N.C., Lau, W.K-M. & Yasunari T.J. Satellite observations of desert dust-induced Himalayan snow darkening, Geophys. Res. Lett., 40, 988–993, doi:10.1002/grl.50226, 2013.

Gorbushina, A.A., Kort, R., Schulte, A., Lazarus, D., Schnetger, B., Brumsack, H.-J., Broughton, W.J. & Favet, J. Life in Darwin's dust: intercontinental transport and survival of microbes in the nineteenth century, Environ. Microbiol., 9,12, 2911–2922, 2007.

Grenfell, T. C., Warren, S. G. & Mullen, P. C. Reflection of solar radiation by the Antarctic snow surface at ultraviolet, visible, and near-infrared wavelengths, J. Geophys. Res., 99,D9,18 669–18 684, 1994.

Hadley, O. & Kirchstetter, T. Black-carbon reduction of snow albedo, Nature Climate Change 2, 437–440, doi:10.1038/nclimate1433, 2012.

Hagler, G. S. W., Bergin, M. H., Smith, E. A. & Dibb, J.E. A summer time series of particulate carbon in the air and snow at Summit, Greenland, J. Geophys. Res., 112, D21309, doi:10.1029/2007JD008993, 2007.

Hansen, J.E. & Hovenier, J.W. Interpretation of the polarization of Venus, J. Atmos. Sci., 31, 1137-1160, doi:10.1175/1520-0469, 1974.

Hansen, J. & Nazarenko, L. Soot climate forcing via snow and ice albedos, Proc. Natl. Acad. Sci., 101, 423–428, doi:10.1073/pnas.2237157100, 2004.

Harris, R. Satellite remote Sensing, An Introduction, Routledge & Kegan Paul, London and New York, ISBN 0-7102-0305-5, 220 p, 1987.

Hegg, D. A., Warren, S. G., Grenfell, T. C., Doherty, S. J. & Clarke, A. D. Sources of light-absorbing aerosol in Arctic snow and their seasonal variation, Atmos. Chem. Phys., 10, 10923–10938, doi:10.5194/acp-10-10923-2010, 2010.

Heikkilä, A. Methods for assessing degrading effects of UV radiation on materials, PhD Thesis. FMI Contributions No 111, ISBN 978-951-697-844-7, 2014.

Hienola, A. I., Pietikäinen, J.-P., Jacob, D., Pozdun, R., Petäjä, T., Hyvärinen, A.-P., Sogacheva, L., Kerminen, V.-M., Kulmala, M. & Laaksonen, A. Black carbon concentration and deposition estimations in Finland by the regional aerosol–climate model REMO-HAM, Atmos. Chem. Phys., 13, 4033-4055, doi:10.5194/acp-13-4033-2013, 2013.

Hudson, S. R., Warren, S.G., Brandt, R.E., Grenfell, T.C. & Six, D. Spectral bidirectional reflectance of Antarctic snow: Measurements and parameterization, J. Geophys. Res.,111, D18106, doi:10.1029/2006JD007290, 2006.

IPCC the Fifth Assessment Report of the Intergovernmental Panel on Climate Change [Stocker, T.F., D. Qin, G.-K. Plattner, M. Tignor, S.K. Allen, J. Boschung, A. Nauels, Y. Xia, V. Bex and P.M. Midgley (eds.)]. Cambridge University Press, Cambridge, United Kingdom and New York, NY, USA, 2013.

Jiao, C., Flanner, M.G., Balkanski, Y., Bauer, S.E., Bellouin, N., Berntsen, T.K., Bian, H., Carslaw, K.S., Chin, M., De Luca, N., Diehl, T., Ghan, S.J., Iversen, T., Kirkevåg, A., Koch, D., Liu, X., Mann, G.W., Penner, J.E., Pitari, G., Schulz, M., Seland, Ø., Skeie, R.B., Steenrod, S.D., Stier, P. , Takemura, T.. Tsigaridis, K., van Noije, T., Yun, Y. & Zhang, K. An AeroCom assessment of black carbon in Arctic snow and sea ice, Atmos. Chem. Phys., 14, 2399-2417, doi:10.5194/acp-14-2399-2014, 2014.

Järvi, J., Hannuniemi, H., Hussein, T., Junninen, H, Aalto, P. P., Hillamo R., Mäkelä T., Keronen P., Iivola E., Vesala T. & Kulmala M. The urban measurement station smear iii: continuous monitoring of air pollution and surface–atmosphere interactions in Helsinki, Finland, Boreal Env. Res., 14 (suppl. a): 86–109, 2009.

Kaspari, S., McKenzie Skiles, S., Delaney, I., Dixon, D. & Painter, T.H. Accelerated glacier melt on Snow Dome, Mount Olympus, Washington, USA, due to deposition of black carbon and mineral dust fromwildfire, J. Geophys. Res. Atmos., 120, 2793–2807, doi:10.1002/ 2014JD022676, 2015.

Kelly, L.C., Cockell, C.S., Thorsteinsson, T., Marteinsson, V. & Stevenson, J. Pioneer Microbial Communities of the Fimmvörðuháls Lava Flow, Eyjafjallajökull, Iceland, Microbial Ecology 1-15, doi:10.1007/s00248-014-0432-3, 2014.

Knippertz, P. & Stuut, J.-P. (eds.). Mineral Dust – a key player in the Earth System, Springer, ISBN 978-94-017-8978-3, doi:10.1007/978-94-017-8978-3, 2014.

Koch, D. & Del Genio, A. D., Black carbon semi-direct effects on cloud cover: review and synthesis, Atmos. Chem. Phys., 10, 7685-7696, doi:10.5194/acp-10-7685-2010, 2010.

Koch, D. & Hansen, J. Distant origins of Arctic black carbon, A Goddard Institute for Space Studies ModelEexperiment, J. Geophys. Res.,110, D04204, doi:10.1029/2004JD005296, 2005.

Kokhanovsky, A.A. & Leeuw, G. (eds). Satellite Aerosol Remote Sensing Over Land. Springer, ISBN 978-3-540-69396-3, 2009.

Kuusisto, E. Snow accumulation and snowmelt in Finland.Helsinki, Publications of the water Research Institute 55, ISBN 951-46-7494-4, 149 p., 1984.

Laborde, M., Crippa, M., Tritscher, T., Jurányi, Z., Decarlo, P. F.,Temime-Roussel, B., Marchand, N., Eckhardt, S., Stohl, A., Baltensperger, U., Prévôt, A. S. H., Weingartner, E. & Gysel, M., Black carbon physical properties and mixing state in the European megacity Paris, Atmos. Chem. Phys., 13, 5831–5856, doi:10.5194/acp-13-5831-2013, 2013.

Li, W., Stamnes, K., Eide, H. & Spurr, R. Bidirectional reflectance distribution function of snow: Corrections for the Lambertian assumption in remote sensing applications, Optical Engineering 46(6), doi:10.1117/1.2746334, 2007.

Liou, K.N. An Introduction to Atmospheric Radiation, Academic Press; 583 p., 2002.

Lutz, S., Anesio, A.M., Raiswell, R., Edwards, A., Newton, R.J., Gill, F. & Benning, L.G.The biogeography of red snow microbiomes and their role in melting arctic glaciers, Nature Communications, 7:11968 doi: 10.1038/ncomms11968, 2016.

Manninen, T. & Roujean, J-L. SNORTEX, Snow Reflectance Transition Experiment, https://helda.helsinki.fi/bitstream/handle/10138/135970/2014nro7.pdf?sequence=1978-951-697-835-5, ISBN 978-951-697-835-5, Unigrafia Helsinki 2014.

Mayer, B. & Kylling, A. Technical note: The libRadtran software package for radiative transfer calculations – description and examples of use, Atmos. Chem. Phys., 5, 1855–1877, doi:10.5194/acp-5-1855-2005, 2005.

McConnell, J.R., Edwards, R., Kok, G.L., Flanner, M.G., Zender, C.S., Saltzman, E.S., Banta, J.R., Pasteris, D.R., Carter, M.M. & Kahl, J.D.W. 20th century industrial black carbon emissions altered Arctic climate forcing, Science, August 9, 2007, doi: 10.1126/science.1144856, 2007.

McKinlay, A. F. & Diffey, B. L. A reference action spectrum for ultraviolet induced erythemal in human skin. Human Exposure to Ultraviolet Radiation: Risks and Regulations, W. R. Passchler & B. F. M. Bosnajakovic, Eds., Elsevier, 83–87, 1987.

McNeill, V. F., Grannas, A. M., Abbatt, J. P. D., Ammann, M., Ariya, P., Bartels-Rausch, T., Domine, F., Donaldson, D. J., Guzman, M. I., Heger, D., Kahan, T. F., Klan, P., Masclin, S., Toubin,C. & Voisin, D. Organics in environmental ices: sources, chemistry, and impacts, Atmos. Chem. Phys., 12, 9653–9678, doi:10.5194/acp-12-9653-2012, 2012.

Meinander, O., Wuttke, S., Seckmeyer, G., Kazadzis, S., Lindfors, A. & Kyrö, E. Solar Zenith Angle Asymmetry Cases in Polar Snow UV Albedo, Geophysica, 45, 1–2, 183–198, 2009.

Mie, G. Beiträge zur Optik trüber Medien, speziell kolloidaler Metallösungen.Annalen der Physik, 330, 3,377–445, ISSN 1521-3889, doi:10.1002/andp.19083300302, 1908.

Myhre, G., Shindell, D., Bréon, F.-M., Collins, W., Fuglestvedt, J., Huang, J., Koch, D.,. Lamarque, J.-F , Lee, D., Mendoza, B. , Nakajima, T., Robock, A., Stephens, G., Takemura, T. & Zhang, H., Anthropogenic and Natural Radiative Forcing. In: Climate Change 2013: The Physical Science Basis. Contribution of Working Group I to the Fifth Assessment Report of the Intergovernmental Panel on Climate Change [Stocker, T.F., D. Qin, G.-K. Plattner, M. Tignor, S.K. Allen, J. Boschung, A. Nauels, Y. Xia, V. Bex and P.M. Midgley (eds.)]. Cambridge University Press, Cambridge, United Kingdom and New York, NY, USA, 2013.

Nordenskiöld, A.E. Nordenskiöld on the inland ice of Greenland, Science, 2, 44, 732-738, doi: 10.1126/science.ns-2.44.732, 1883.

Nousiainen, T. & Kandler, K. Light scattering by atmospheric mineral dust particles, in: Light Scattering Reviews 9, edited by: Kokhanovsky, A. A., Springer Praxis Books, Springer, Berlin, 2015. Heidelberg, 3–52, doi:10.1007/978-3-642-37985-7, 2015.

Painter, T. H., Barrett, A. P., Landry, C. C., Neff, J. C., Cassidy, M. P., Lawrence, C. R., McBride, K. E. & Farmer, G. L. Impact of disturbed desert soils on duration of mountain snow cover, Geophys. Res. Lett., 34, L12502, doi:10.1029/2007GL030284, 2007.

Peltoniemi, J. I., Gritsevich, M., Hakala, T., Dagsson-Waldhauserová, P., Arnalds, Ó., Anttila, K., Hannula, H.-R., Kivekäs, N., Lihavainen, H., Meinander, O., Svensson, J., Virkkula, A. & de Leeuw, G. Soot on Snow experiment: bidirectional reflectance factor measurements of contaminated snow, The Cryosphere, 9, 2323-2337, doi:10.5194/tc-9-2323-2015, 2015.

Perovich, D. K., Grenfell, T. C., Light, B. & Hobbs, P. V. Seasonal evolution of the albedo of multiyear Arctic sea ice, J. Geophys. Res., 107,C10, 8044, doi:10.1029/2000JC000438, 2002.

Pirazzini, R. Surface albedo measurements over Antarctic sites in summer, J. Geophys. Res., 109, D20118, doi:10.1029/2004JD004617, 2004.

Pithan, F. & Mauritsen, T. Arctic amplification dominated by temperature feedbacks in contemporary climate models, Nature Geosci., 7, 181–184, doi:10.1038/ngeo2071, 2014.

Polashenski, C.M., Dibb, J.E., Flanner, M.G., Chen, J.Y., Courville, Z.R., Lai, A.M., Schauer, J.J., Shafer M.M. & Bergin, M. Neither dust nor black carbon causing apparent albedo decline in Greenland's dry snow zone; implications for MODIS C5 surface reflectance, Geophys. Res. Lett., 42, 9319–9327, doi: 10.1002/2015GL065912, 2015.

Prospero, J.M., Bullard, J.E. & Hodgkins, R. High-Latitude Dust Over the North Atlantic: Inputs from Icelandic Proglacial Dust Storms, Science, 335, 1078, doi: 10.1126/Science.13217447, 2012.

Ramanathan, V. & Carmichael, G. Global and regional climate changes due to black carbon, Nature Geoscience 1, 221 – 227, doi:10.1038/ngeo156, 2008.

Robinson, P.J. & Davies, J.A. Laboratory Determinations of Water Surface Emissivity, Journal of Applied Meteorology, 11,8,1391-1392, doi: 10.1175/1520-0450(1972)011<1391:LDOWSE>2.0.CO;2, 1972.

Räisänen, P., Kokhanovsky, A., Guyot, G., Jourdan, O. & Nousiainen, T. Parameterization of single-scattering properties of snow, The Cryosphere, 9, 1277-1301, doi:10.5194/tc-9-1277-2015, 2015.

Sand, M., Berntsen, T., Kay, J.E., Lamarque, J.F., Seland O. & Kirkevag, A. The Arctic response to remote and local forcing of black carbon, Atmos. Chem. Phys., 13, 211-224, 2013.

Schaepman-Strub, G., Schaepman, M.E., Painter, T.H., Dangel, S. & Martonchik, J.V. Reflectance quantities in optical remote sensing—definitions and case studies, Remote Sensing of Environment 103, 27-42, 2006.

Schwarz, J.P., Spackman, J.R., Gao, R.S., Watts, L., Stier, P., Schulz, M., Davis, S.M., Wofsy S.C. & Fahey, D.W. Global-scale black carbon profiles observed in the remote atmosphere and compared to model, Geophys. Res. Lett., 37:L18812, doi:10.1029/2010gl044372, 2010.

Schwarz, J. P., Gao, R. S., Perring, A. E., Spackman, J. R. & Fahey, D. W. Black carbon aerosol size in snow, Scientific Reports, doi:10.1038/srep01356, 2013.

Seckmeyer, G., Bais, A., Bernhard, G., Blumthaler, M., Booth, R.S., Lantz, K. & McKenzie, R. L. Instruments to measure solar ultraviolet radiation, part II: Broadband instruments measuring erythemally weighted solar irradiance, WOM-GAW report, 2005.

Serreze, M. C. & Barry, R. G. Processes and impacts of Arctic amplification: A research synthesis, Global and Planetary Change 77, 85-96, doi:10.1016/j.gloplacha.2011.03.004, 2011.

Setlow, R.B. The wavelengths in sunlight effective in producing skin cancer: a theoretical analysis, Proc. Nat. Acad. Sci., USA, 71, No. 9, 3363-3366, 1974.

Sharma, S., Ishizawa, M., Chan, D., Lavoué, D., Andrews, E., Eleftheriadis, K. & Maksyutov, S. 16-year simulation of Arctic black carbon: transport, source contribution, and sensitivity analysis on deposition, J. Geophys. Res., 118, 1-22. doi:10.1029/2012JD017774, 2013.

Shettle, E. P. Models of aerosols, clouds and precipitation for atmospheric propagation studies, paper presented at Conference on Atmospheric Propagation in the UV, Visible, IR and MM-Region and Related System Aspects, NATO Adv. Group for Aerosp. Res. and Dev., Copenhagen, 1989.

Smolskaia, I., Nunez, M. & Kelvin, M. Measurements of Erythemal Irradiance near Davis Station, Antarctica: Effect of. Inhomegeneous Surface Albedo, Geophys. Res. Lett., 26, 1381–1384, 1999.

Sofiev, M., Galperin, M. & Genikhovich, E. Construction and evaluation of Eulerian dynamic core for the air quality and emergency modeling system SILAM, in: NATO Science for piece and security Serties C: Environmental Security, Air pollution modelling and its application, XIX, edited by: Borrego, C. and Miranda, A. I., Springer, 699–701, 2008.

Stohl, A., Klimont, Z., Eckhardt, S., Kupiainen, K., Shevchenko, V.P., Kopeikin, V.M. & Novigatsky, A.N. Black carbon in the Arctic: the underestimated role of gas flaring and residential combustion emissions, Atmos. Chem. Phys., 13, 8833-8855, 2013.

Sturm, M., Holmgren, J. & Liston, G. E. A seasonal snow cover classification system for local to global applications, J. Clim., 8, 1261–1283, 1995.

Svensson, J., Ström, J., Hansson, M., Lihavainen, H. & Kerminen, V.-M. Observed metre scale horizontal variability of elemental carbon in surface snow, Environmetal research Letters, 8, doi:10.1088/1748-9326/8/3/034012, 2013.

Svensson, J., Virkkula, A., Meinander, O., Kivekäs, N., Hannula, H.-R., Järvinen, O., Peltoniemi, J., Gritsevich, M., Heikkilä, A., Kontu, A., Neitola, K., Brus, D., Dagsson-Waldhauserova, P., Anttila, K., Vehkamäki, M., Hienola, A., Leeuw, G. & Lihavainen, H. Soot-doped natural snow and its albedo — results from field experiments, Boreal Env. Res., 21, 481–503, 2016.

Tanskanen, A. & Manninen, T. Effective UV surface albedo of seasonally snow-covered lands, Atmos. Chem. Phys., 7, 2759–2764, 2007.

Tedesco, M., Doherty, S., Warren, S., Tranter, M., Stroeve, J., Fettweis, X. & Alexander, P. What darkens the Greenland Ice Sheet?, Eos, 96, doi:10.1029/2015EO035773,2015.

Tirsch, D., Craddock, R. A., Platz, T., Maturilli, A., Helbert, J. & Jaumann, R. Spectral and petrologic analyses of basaltic sands in Ka'u Desert (Hawaii) – implications for the dark dunes on Mars, Earth Surf. Process. Landforms, 37, 434–448, doi: 10.1002/esp.2266, 2012.

Trenberth, K.E., Jones, P.D., Ambenje, P., Bojariu, R., Easterling, D., Tank, A.K., Parker, D., Rahimzadeh, F., Renwick, J.A., Rusticucci, M., Soden, B. & Zhai, P. Observations: surface and atmospheric climate change. In Climate Change 2007: The Physical Science Basis, edited by S. Solomon, D. Qin, M. Manning, Z. Chen, M. Marquis, K. B. Averyt, M.Tignor & H. L. Miller. Cambridge, United Kingdom and New York, N.Y., USA: Cambridge University Press, 2007.

UNEP.Environmental Effects of Ozone Depletion: 2002, Assessment, United Nations Environment Programme. ISBN 92-807-2312-X, http://www.unep.org/OZONE/pdf/eeap-report2002.pdf, 2002.

Voisin, D., Jaffrezo, J.-L., Houdier, S., Barret, M., Cozic, J., King, M. D., France, J. L., Reay, H. J., Grannas, A., Kos, G., Ariya, P. A., Beine, H. J. & Domine, F. Carbonaceous species and HUmic LIke Substances (HULIS) in Arctic snowpack during OASIS field campaign in Barrow, J. Geophys. Res., 117, D00R19, doi:10.1029/2011JD016612, 2012.

Wang, R., Tao, S., Balkanski, Y., Ciais, P., Boucher, O., Liu, J., Piao, S., Shen, H., Raffaella Vuolo, M., Valari, M., Chen, H., Chen, Y., Cozic, A., Huang, Y., Li, B., Li, W., Shen, G., Wang B. & Zhang, Y. Exposure to ambient black carbon derived from a unique inventory and high-resolution model, PNAS, vol. 111 no. 7, 2459–2463, doi: 10.1073/pnas.1318763111, 2014.

Warren, S. G. Can black carbon in snow be detected by remote sensing?, J. Geophys. Res. Atmos., 118, 779–786, doi:10.1029/2012JD018476,2013.

Warren, S. & Wiscombe, W. A Model for the Spectral Albedo of Snow. II: Snow Containing Atmospheric Aerosols, Journal of the Atmospheric Sciences, 37, 12, 2734-2745, doi: http://dx.doi.org/10.1175/1520-0469(1980)037<2734:AMFTSA>2.0.CO;2, 1980.

Webb, A., Grobner, J. & Blumthaler, M. A practical guide to operating broadband instruments measuring erythemally weighted irradiance, WMO SAG UV, COST-726, ISBN 92-898-0032-1, 2006.

Weller, G. The tundra microclimate during snow-melt at Barrow, Alaska, Arctic, 25, 291–299, 1972.

WHO. Solar ultraviolet radiation: global burden of disease from solar ultraviolet radiation, Environmental burden of disease series, No. 13. World Health Organization.ISBN 92 4 159440 3, 2006.

Wiscombe, W. J. & Warren, S. G. A model for the spectral albedo of snow. I: Pure snow, J. Atmos. Sci., 37, 2712–2733, 1980.

Wuttke, S., Seckmeyer, G. & Ḱonig-Langlo, G. Measurements of spectral snow albedo at Neumayer, Antarctica, Ann. Geophys., 24, 7–21, 2006.

WMO. Instruments to Measure Solar Ultraviolet Radiation, Part 1: Spectral Instruments (lead author G. Seckmeyer) (WMO TD No. 1066), 2001.

WMO. Guide to Meteorological Instruments and methods of Observation, WMO-No. 8 (Seventh Edition,6 August 2008), http://www.wmo.int/pages/prog/www/IMOP/publications/CIMO-Guide/CIMO Guide-7th Edition-2008.html, 2008.

WMO. GAW Report No. 212, Standard Operating Procedures (SOPs) for Spectral Instruments Measuring Spectral Solar Ultraviolet Irradiance, http://www.wmo.int/pages/prog/arep/gaw/documents/Final_GAW_212.pdf, 2014.

Zhang, J., Liu, J., Tao, S. & Ban-Weiss, G. A. Long-range transport of black carbon to the Pacific Ocean and its dependence on aging timescale, Atmos. Chem. Phys., 15, 11521-11535, doi:10.5194/acp-15-11521-2015, 2015.